Numerical and functional representations of regional heat flow in South America

Valiya M. Hamza [a,*], Fernando J.S. Silva Dias [a], Antonio J.L. Gomes [a],
Zenón G. Delgadilho Terceros [b]

[a] *Observatório Nacional – ON/MCT, Rua General José Cristino, 77, Rio de Janeiro, Brazil*
[b] *Empresa Nacional de Eletricidad S.A. "ENDE", Proyecto Geotérmico Laguna Colorada, Cochabamba, Bolivia*

Abstract

A summary of heat flow data acquired over recent years in several areas in the eastern (Brazil and Paraguay) and western (Bolivia, Chile, Colombia and Ecuador) parts of South American continent are presented. The improvements in the database have allowed numerical representations of heat flow for southeastern and central segments of the Precambrian fold belts in Brazil, Central Andean cordilleras in Chile and Bolivia, Southern Volcanic arc in Peru, Neuquén Province in southwestern Argentina, Chaco basin in Paraguay, Oriente basin in Ecuador and the system of pericratonic basins in north central Colombia. The maps reveal considerable variability in heat flow, not only between the main tectonic units but also within them. The intra-regional variations seem to originate mainly from complexities in local geologic structures while the inter-regional ones seem to point to action of deep-seated tectonic processes. The cordilleran regions are, in general, characterized by relatively high heat flow (>70 mW/m^2), compared with the coastal regions to the west and the Pre-cordilleran basins to the east. In the eastern part of the continent, heat flow is low to normal (<60 mW/m^2), the exceptions being the Mesozoic rift basins, areas of Cenozoic alkaline intrusions and some isolated belts of overthrust tectonics in the central parts of Brazil. There are indications that heat flow is high in the Patagonian Platform relative to that found in the Brazilian Platform.

In addition, polynomial methods were employed for examining large-scale variations of heat flow over the continent. Specifically, a general-purpose least square solution was used to determine the coefficients of up to fourth order in latitude and longitude. Some of the large-scale trends seen in low order polynomial representations seem to be indicative of the nature of deep-seated heat transfer processes. The systematic increase in regional heat flow in the north-south direction is an example. It is considered as the consequence of thermal blanketing effect of the continental segment of the South American lithosphere. Trends seen in higher order polynomials seem to be associated with regional tectonic patterns and subduction-related magmatism. Prominent among these are east-west trending belts of low heat flow in northern Peru and in central Chile, as well as the high heat flow belts in northern Chile, Altiplano of Bolivia and northwestern Argentina. Limitations arising from low data density and uneven geographic distribution warrant higher degree polynomial representations.
© 2005 Elsevier B.V. All rights reserved.

Keywords: Heat flow; Regional maps; South America; Polynomial representation

---

* Corresponding author. Tel.: +55 21 2580 7081.
  E-mail addresses: hamza@on.br (V.M. Hamza), fernando@on.br (F.J.S.S. Dias), ajlgomes@on.br (A.J.L. Gomes), z_delgadillo@hotmail.com (Z.G.D. Terceros).

1. Introduction

A considerable body of geothermal data has been acquired over South America during the last few decades, but very few efforts have so far been made in obtaining functional representations of regional heat flow field of the continent. Poor knowledge of regional heat flow field has been an obstacle in understanding large-scale thermal features of the South American plate. Hamza and Muñoz (1996), in presenting the manual and automatic contour maps of heat flow of the South American continent, pointed out low data density and uneven geographic distribution as the main obstacles in outlining the regional geothermal fields. It is therefore of paramount importance to extract as much information as possible concerning heat flow on local and regional scales.

An updated database has been setup for this purpose, which include mainly information on temperature gradients, thermal conductivity and heat flow. In addition, a careful evaluation of the data reported in earlier compilations has been carried out. The regions for which new geothermal data has been acquired include several areas in the eastern (Brazil and Paraguay) and western (Argentina, Bolivia, Chile, Colombia and Ecuador) parts of the continent. Comparison with previous compilations indicates that there have been some improvements in data quality. Thus, results obtained by conventional methods constitute a significant part of the data set in the central and eastern parts of the continent. Low quality estimates based on complementary geological and geochemical data are retained only for areas of poor data density in the southwestern and northern parts of the Andean region. The geographic distribution, however, continue to be non-uniform, there being several tectonic units in the northern parts of the continent (mainly in the Amazon region, Surinam and the Guianas) for which hardly any geothermal data are available.

The improvements in data density and quality have opened up possibilities for mapping heat flow in local and regional scales. The approach adopted in the present work has been to make use of numerical representations of heat flow fields on local and regional scales and polynomial representations on continental scale. A variety of contouring schemes were tested using commercially available software packages that allow such methods as linear, nearest neighbor, kernel smoothing, weighted fill and kriging for data interpolation. In the present case, where data density is low and its distribution non-uniform, interpolation schemes based on weighted fill and kriging were preferred in producing contour maps. Such maps are useful in illustrating regional variations. However, it is convenient to note that numerical schemes employed in common map contouring packages are based on interpolated values at regular grid points, which leads to some enhancement of the lateral dimensions of the anomalies in areas of low data density. One of the convenient means of overcoming this problem is to make use of empirical predictors for estimating heat flow for grid elements where experimental data are not available. Nevertheless, such procedures need to be adopted with caution as it introduces subjective estimates into the numerical mapping scheme.

We present first a brief overview of the main features of the data acquired in recent years. This is accompanied by regional heat flow maps, which are numerical representations based on the updated data sets. Polynomial methods were employed for examining large-scale variations of heat flow over the continent. Specifically, a general-purpose least square solution was used to determine the coefficients of up to sixth order in latitude and longitude. Maps of low and higher order trend surfaces as well as that of residual anomalies are presented in the last section.

2. Characteristics of the updated data base

Hamza and Muñoz (1996) reported a compilation consisting of 655 heat flow values. It included not only heat flow determinations by conventional methods for 432 localities but also estimates of heat flow by the relatively low quality geochemical methods for some 223 additional sites. New data acquired since this earlier compilation include conventional heat flow measurements in the Central Andean cordilleras and highlands in Bolivia and Chile (Springer and Foerster, 1998), Copahue area in southwestern Argentina (Mas et al., 2000) and selected localities in the central and coastal region of the Brazilian Platform (Ferreira, 2003; Gomes, 2003). Also chemical analyses of thermal springs, useful for estimates of terrestrial heat flow by geochemical methods, have been carried out in southwestern Colombia (Alfaro and Bernal, 2000) and Southern Cordillera of Peru (Steinmuller, 2001). Other related geothermal data sets reported in the literature include bottomhole temperatures in oil wells of the Chaco Plains in Paraguay (Kuhn, 1991; Wiens, 1995), Marañon basin in Peru (Mathalone and Montoya, 1995), Oriente basin in Ecuador (Smith, 1989) and pericratonic basins in central Colombia (Alfaro et al., 2000). These data sets have allowed determination of heat flow for 159 localities and estimates for additional 26 sites.

A summary of the updated database for South America is presented in Table 1a, indicating its distribution among the thirteen countries in the continent. Heat flow

Table 1a
Present status of heat flow data distribution in the South American countries

Country	Area (km^2)	Number of data		Data density (per 10^6 km^2)	
		Hamza and Muñoz (1996)	This work	Hamza and Muñoz (1996)	This work
Argentina	2,776,889	63	63	23	23
Bolivia	1,098,581	37	52	34	47
Brazil	8,511,965	388	434	45	51
Chile	756,945	45	56	59	74
Colombia and Panama	1,215,996	12	34	10	28
Ecuador	283,561	1	30	4	106
French Guiana	91,000	–	–	–	–
Guiana	214,969	–	–	–	–
Paraguay	406,752	–	35	–	86
Peru	1,285,216	69	96	54	75
Suriname	163,265	–	–	–	–
Uruguay	177,508	–	–	–	–
Venezuela	912,050	40	40	44	44
Total	17,817,615	655	840	37	46

values are now available for nine out of thirteen countries, the exceptions being French Guiana, Guiana and Suriname in the north and Uruguay in the south. The updated data set consists of 840 heat flow values of which 591 are direct determinations while 249 are indirect estimates. Compared to the previous compilation reported by Hamza and Muñoz (1996) the number of heat flow values based on the conventional and BHT methods have increased from 432 to 591, constituting thereby a significant improvement in data quality. Fig. 1 illustrates the geographic distribution of the updated data set. Also indicated in this figure are the areas where new geothermal data have been acquired. As can be noted, the new heat flow values have lead to some improvements in the geographic distribution. The overall data density is about 45 per million square kilometers, comparable to data densities reported for several parts of Europe at the time preparation of the first continental heat flow map (Cermak and Hurtig, 1979).

The quality of the data set is however, variable, consisting of values obtained using conventional methods as well as estimates based on complementary geochemical data. The distribution of the methods used for heat flow determinations in the different countries is given in Table 1b. Heat flow values by conventional and bottom-hole temperature (BHT) methods constitute major parts of the data set for Bolivia, Brazil, Colombia, Ecuador, Paraguay and Peru. On the other hand, estimates by the relatively low quality geochemical methods (Swanberg and Morgan, 1979) continue to represent significant parts of the database for Argentina, Chile and Venezuela. The limitations imposed by the available data set are obvious and the extent to which such features represent true vari-

ations in the regional geothermal field depends on how representative the data are of the deep thermal regime. This problem is intimately related to the specific nature of data set and further advances can be achieved only with improvements in both the quality and quantity of the database. However, setting any specific rule concerning the reliability of the final calculated heat flow values
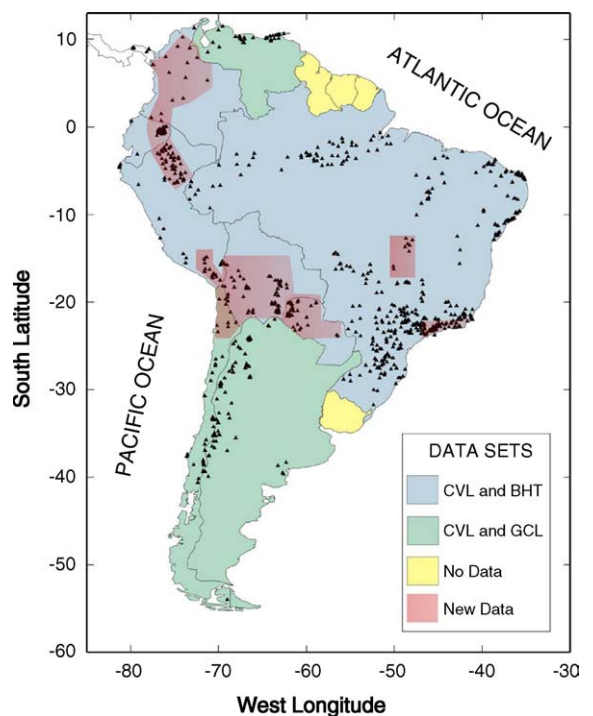

Fig. 1. Geographic distribution of heat flow data in South America. Color codes indicate characteristics of the data set. See text for details.

Table 1b
Summary of methods used for heat flow determinations in South America

Country	Methods of heat flow determination						Total
	CVL	BHT	AQT	MGT	GCL	OHF	
Argentina	4	1	–	–	58	–	63
Bolivia	10	32	–	10	–	–	52
Brazil	129	189	13	4	99	–	434
Chile	15	6	–	–	35	–	56
Colombia and Panama	12	14	–	–	8	–	34
Ecuador	1	29	–	–	–	–	30
Paraguay	–	35	–	–	–	–	35
Peru	13	52	–	3	9	19	96
Venezuela	–		–	–	40	–	40
Total	184	358	13	17	249	19	840

CVL, conventional; BHT, bottom hole temperature (includes CBT, conventional bottom temperature); AQT, aquifer temperature; MGT, underground mine; GCL, geochemical; OHF, oceanic heat flow. See text for details.

is a difficult task, as the measurement techniques and data acquisition procedures have changed significantly over the years.

At this point, some comments on the procedures adopted in acquisition and analysis of geothermal data are in order. Most of the measurements in hard rock terrains have been carried out using conventional methods. On the other hand, those in sedimentary basins are based largely on bottom-hole temperature (BHT) data sets. Our experience indicates that data acquired as part of exploration activities by mining and oil companies do not often meet the quality requirements for scientific investigations. In addition, several of the data sets used for geothermal studies in South America are of restricted access, unavailable for independent analysis. Primary sources of data sets published by Springer and Foerster (1998), the ones mentioned by Alfaro et al. (2000) and classified reports mentioned in the work of Husson and Moretti (2002) are examples. Proliferation of gradient values based on classified reports, unavailable for scientific scrutiny, point to the need for setting up a public domain geothermal database for South America.

Another problem refers to the availability of thermal property data. In many of the earlier works (see, for example, Uyeda et al., 1978; Watanabe et al., 1980; Henry and Pollack, 1988) the approach has been such that the geological aspects of thermal properties were considered largely as *secondary*. Near total absence of relevant information on rock types and lithologic sequences, common in many of the earlier publications and reports, point to this aspect of the problem. Another aggravating factor in this context is the lack of systematic efforts for experimental determination of thermal properties of the main geologic formations in South America. As a result, the availability of suitable thermal property

data is extremely limited, making new attempts at determination of heat flow a difficult task.

Efforts have been made in recent years to attenuate this problem by carrying out thermal property measurements of a number of geologic formations, mainly in the southern and central parts of Brazil. Thus, laboratory measurements of thermal properties have been carried out on over 2000 rock samples representative of several of the major geologic formations in southern and central Brazil. In addition, information available in the literature, that are of potential help in obtaining first order estimates of thermal conductivity, have also been compiled. This compilation includes results of mineral analyses, stratigraphic correlation charts and seismic sections of sedimentary basins. Results of chemical analyses and mineral composition in conjunction with tabulated data for minerals (see, for example, Horai and Simmons, 1969) have been used for obtaining first order estimates of effective thermal conductivity of igneous and metamorphic rocks. Similarly, stratigraphic sections with information on thickness and rock type were used in conjunction with tabulated data (see, for example, Kappelmeyer and Haenel, 1974) in evaluating effective thermal conductivity of sedimentary rock formations. Such estimates of thermal conductivity have allowed determination of heat flow in areas where only temperature gradient data were previously available. The overall benefit of such an approach is that the critical problems (gridding and interpolation) in preparation heat flow maps for areas of low data density may be minimized. In a more fundamental sense, the approach is similar to the use of empirical predictors employed in global heat flow maps (Chapman and Pollack, 1975; Pollack et al., 1993).

A number of different experimental techniques have been employed in the acquisition of new data sets, a nat-

ural consequence of the recent advances in technology and instrumentation. Details of the procedures employed in temperature and conductivity measurements as well as determination of geothermal gradients and heat flow are presented in Appendix A. Given below are brief descriptions of the results for eight major tectonic regions of the South American continent.

2.1. Coastal area of southeastern Brazil

The metamorphic fold belts of the Brasiliano orogenic cycle constitute the basement rocks of the coastal area of southeastern Brazil. With the exception of tectonic movements associated with the development of shallow basins during Paleozoic the region in the interior parts of the Brazilian Platform has been tectonically quiescent since the Precambrian times. The coastal area has however undergone vertical movements associated with opening of the Atlantic Ocean, since the Cretaceous. Another notable feature is the presence of alkaline intrusive activity during the Tertiary period.

During the period of 1998–2001, new geothermal data were acquired in the coastal area of southeastern Brazil, between latitudes 21°S and 25°S, as part of a project for detailed geothermal investigations of the state of Rio de Janeiro. Activities carried out during the initial phase of this project include temperature logs of suitable boreholes and water wells, determination of thermal gradients and measurements of thermal conductivity of the main rock formations.

Availability of deep bore holes for temperature logs in the inland areas of the states of Rio de Janeiro and São Paulo is rather limited, a consequence of the reduced level of exploratory drilling in this region. Thus, determination of thermal gradients are based on data obtained in temperature logs of shallow bore holes and water wells. Boreholes that have been abandoned for periods of the order of several months to years were selected for this purpose. In many cases, the temperature variations were found to be near linear, generally at depths of greater than the depth of penetration of seasonal changes in surface temperatures. In such cases, thermal gradients were determined by least square fit to data sets selected from appropriate depth intervals. A very brief description of the procedure, designated here as the *conventional method* (CVL), is given in Appendix A. Examples of vertical distributions of temperatures suitable for determining thermal gradients are presented in Fig. 2a. A summary of the relevant data on borehole depths, temperature measurements, gradient values and error estimates are provided in Table 2a. The available data has allowed determination of geothermal gradients in 23 localities.

A number of corrections were applied to the field data, before its use in the determination of temperature gradients. Among these are depth corrections for deviations from the vertical of borehole, thermal transients generated by drilling, effects of topography and perturbations induced by climate changes of the recent past. Deviations from the vertical, of boreholes considered in the present study, were small enough to be negligible. The transient effects of drilling are also found to be insignificant as the time elapsed between cessation of drilling and logging operations are more than several orders of magnitude greater than the duration of drilling. The topographic features in southeastern Brazil are in quasi-steady state as there have been no recent episodes of uplift or subsidence. Thus, the procedures adopted for topographic corrections are based on the steady state model proposed by Bullard (1940). The corrections were found to be significant only for three sites. The perturbations arising from climate and vegetation changes of the recent past were examined using both forward (Birch, 1948) and inverse (Shen and Beck, 1983) modeling procedures. Such corrections were found to be significant only for gradients at shallow depths of less than 100 m, in agreement with results of recent studies by Cavalcante (2003) and Cerrone and Hamza (2003). The sites for which climate corrections were considered are indicated in Table 2a. Lack of deeper bore holes have not allowed estimates of climate perturbations at larger depths, induced by long-term variations in the climate.

In some of the uncased boreholes, non-linear temperature variations were observed, which could not be considered as arising neither from surface temperature variations nor from reasonable changes in thermal conductivity. Thermal refraction effects were also found to be unlikely. Thus, advection heat transport by in-hole fluid flows has been considered as the most probable mechanism inducing such perturbations. Such flows have been found to occur in cases where the boreholes themselves act as interconnecting paths between fracture systems or permeable zones. For example, in reporting geothermal data for boreholes in Salton Sea area, Sass et al. (1988) pointed out advective heat transport by in-hole fluid flows as the most likely mechanism for the presence of non-linear features in temperature profiles.

In such cases, the absence of linearity in temperature profiles does not allow the use of conventional approach for determining thermal gradients by least square fits. The thermal resistance method also fails in such cases, as the non-linear features in temperatures are unrelated to variations in the thermal conductivity. To circumvent this difficulty a procedure designated here as the *conventional bottom temperature method* (CBT), was adopted.
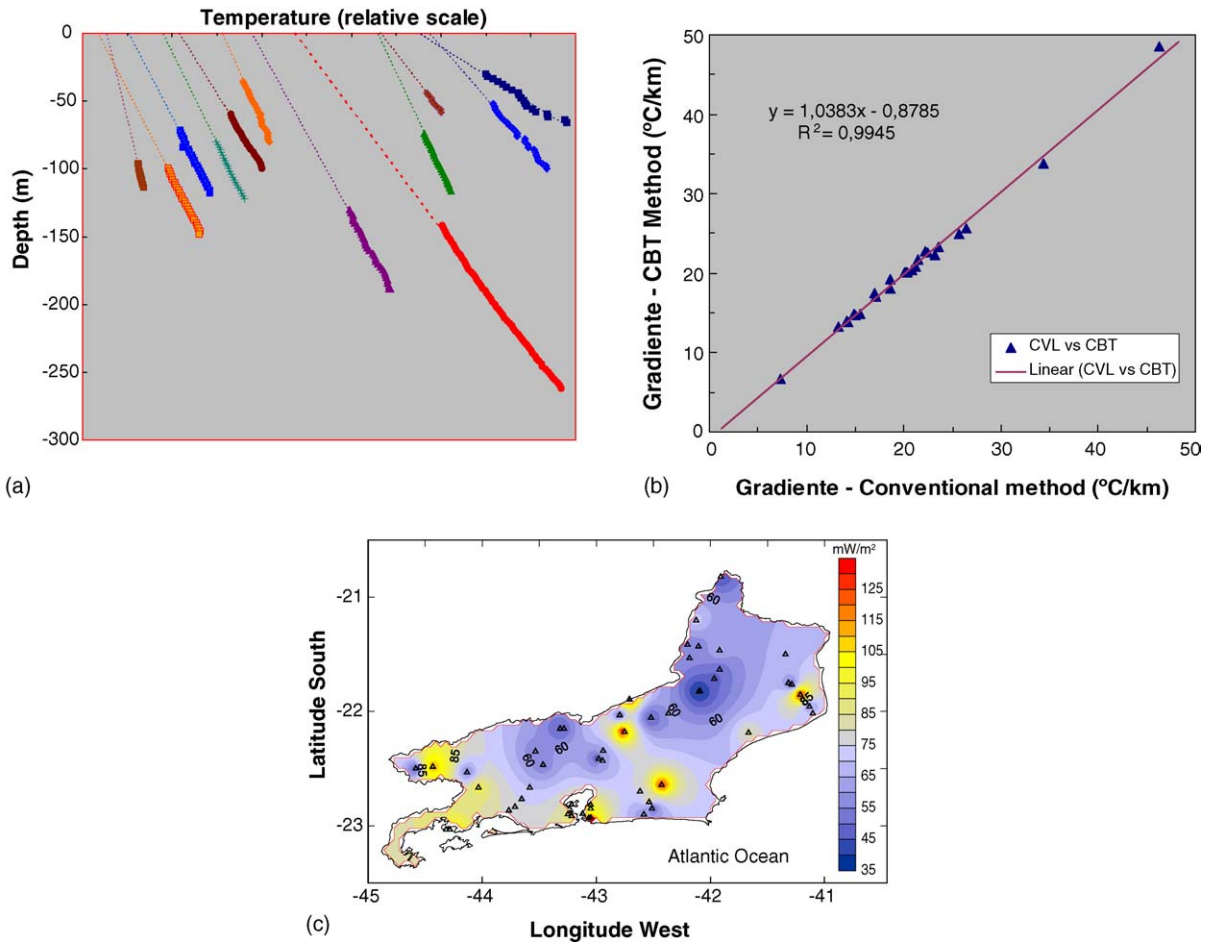
Fig. 2. (a) Illustrative examples of log segments that exhibit near linear variations of temperatures at shallow depths in the southeastern coastal area of Brazil. The relative scale for temperature has the purpose of retaining clarity in presentation. (b) Coorelation between gradients calculated using conventional (CVL) and bottom temperature (CBT) methods, for boreholes located in the southeastern coastal area of Brazil. (c) Heat flow map of the state of Rio de Janeiro, in the southeastern coastal area of Brazil. The triangles indicate locations of heat flow measurements. The numbers on the curves refer to heat flow in mW/m^2.

It makes use of the difference between the bottom temperature of the borehole and the mean annual surface temperature in calculating an *apparent temperature gradient*. The method is essentially the same as the well-known bottom-hole temperature method (Carvalho and Vacquier, 1977), the main difference being the improved accuracy with which bottom temperatures can be determined and the facility with which repeat measurements carried out. It is conceptually simpler, but rather sensitive to errors in the value adopted for the mean annual surface temperature, especially in the case of shallow wells. Implicit in this approach is the assumption that the temperature at the bottom part of the well is less prone to perturbations induced by in-hole water flows. A rigorous test of the reliability of CBT method would require comparative analyses of repeat temperature logs,

carried out before and after blockage of hydraulically active fracture zones in bore-holes. However, cementing operations capable of blocking in-hole flows are expensive and not practical in many cases. Thus, recourse was made to relatively simple procedures that provide indirect checks on the reliability of this method. One such alternative is to compare the gradient values by the CBT method with those obtained by the conventional (CVL) method for undisturbed boreholes, situated in the same general region as that of the boreholes with hydraulic disturbances. Results of such a comparison, presented in Fig. 2b, reveal that the use of CBT method leads to errors of less than 4% in the determination of gradients in the interval of 5–50 °C/km.

In the present case, soil temperature and meteorological data reported in the climate atlas of the state of Rio de

Table 2a
Summary of temperature logs and gradient values obtained using the conventional (CVL) method in the southeastern coastal area of Brazil

Municipality	Identification	Coordinates		N_T	Depth (m)	Gradient (°C/km)	
		Latitude	Longitude			Γ	σ
Campos	Baixa Grande	21.9578	41.9197	55	108	18.6	1.85
	Boa Vista	22.0183	41.1322	50	100	26.4	0.50
	UENF2	21.7636	41.2864	51	100	18.7	0.30
Angra. Reis	Bonfim	23.0333	44.2833	33	66	46.2[a]	2.20
Duas Barras	DBP1	22.0547	42.5203	62	122	14.9[b]	0.20
	DBP2	22.0547	42.5203	34	66	14.9[a,b]	0.10
	DBP3	22.0547	42.5206	40	78	17.0[a,b]	2.56
Maricá	M. Ribeiro	22.0547	42.5206	50	98	20.1[a]	2.63
Miracema	Centro	21.4167	42.2	38	78	20.4[a]	2.56
Niterói	Cafubá	22.9325	43.0672	59	116	14.2	0.10
Paraíba Sul	C. das Almas	22.15	43.3167	51	100	17.1	2.00
Porciúncula	Santa Clara	20.8211	41.9094	41	80	13.3[a]	0.36
Saquarema	Gj. S. Antonio	22.8489	42.5122	60	118	15.0	0.33
S.Seb.do Alto	V. Barro	21.8231	42.0994	59	114	7.3	0.14
Seropédica	Orfanato	22.7661	43.6542	136	262	22.5	0.13
	P.S.Piranema	22.8356	43.7131	61	120	21.5	1.76
Teresópolis	FVM	22.4331	42.9444	69	134	20.9[b]	0.01
	Faz. Texas	22.3442	42.9403	44	68	22.2[a,b]	0.02
	BC2	22.4331	42.9444	75	148	15.6[b]	0.18
	Barra Imbui	22.4142	42.9783	51	100	21.2[b]	0.01
Vassouras	Massambará	22.35	43.5333	36	80	14.1[a,b]	0.06
V. Redonda	Padre Josimo	22.5333	44.1333	22	70	20.3[a]	2.86
Mean	–	–	–	53	104	19.4	0.96

N_T is total number of temperature measurements, Z the depth of the borehole, Γ the least square temperature gradient and σ its standard deviation.

[a] The corrections for climate.

[b] The corrections for topography.

Janeiro (Duarte et al., 1978) were used as proxy for the mean annual surface temperatures. The gradient values obtained using the CBT method are given in Table 2b. The relatively close agreement between the mean values of gradients by conventional (Table 2a) and CBT methods (Table 2b) is considered also as an indication of the reliability of this latter approach.

The methods adopted for thermal conductivity measurements were dictated mainly by the physical characteristics of the available rock samples. For boreholes in the São Sebastião area, in the coastal region of the state of São Paulo, solid core samples were available and measurements were carried out using a locally built and calibrated half space line source device. For wells in the municipality of Campos, in the eastern part of Rio de Janeiro, only drill cuttings were available. Hence measurements were made on water-saturated samples using a conventional needle probe device (Von Herzen and Maxwell, 1959). Conductivity of rock fragments were then calculated following the procedure described by Sass et al. (1971) and making use of the available

porosity data. In cases where neither core samples nor drill cuttings were available, fresh samples were collected from outcrops of rock formations, representative of those encountered in the wells. The thermal conductivity of such samples was measured using a portable plane source device. A brief summary of the measurement procedures are given in the Appendix. Thermal conductivity values were calculated for 21 different rock types occurring within the study area. Gomes (2003) calculated weighted mean thermal conductivity of the main rock types in estimating representative values for the main geological formations and presented a map of thermal conductivity variations in the state of Rio de Janeiro. A summary of the results of thermal conductivity measurements based on these earlier is presented in Table 2c.

The temperature gradient and thermal conductivity values were used in calculating heat flow for 31 sites in southeastern Brazil. The data are classified into three groups depending on the local geological characteristics (Table 2d). As can easily be noted, the heat flow is

Table 2b
Summary of temperature logs and gradient values obtained using the conventional bottom temperature (CBT) method in the southeastern coastal area of Brazil

Municipality	Identification	Coordinates		N_T	Depth (m)	Gradient (°C/km)	
		Latitude	Longitude			Γ	σ
Cambuci	Monte Verde	21.4664	41.9197	43	84	24.7	5.95
Campos	Consel. Josino	21.5006	41.3419	39	76	21.3	6.58
	S. Sebastião	21.8539	41.2111	13	76	21.3	7.69
Carapebus	Centro	22.1869	41.6656	46	90	30.2	5.56
Duas Barras	DBP4	22.0547	42.5206	40	78	16.3	6.41
Itaocara	Cel. Teixeira	21.6333	41.9197	39	76	19.0	6.58
	Jaguarembé	21.7133	41.9667	51	100	17.2	5.00
Itatiaia	Xerox2	22.5000	44.5833	46	90	16.5	5.56
Laje de Muriaé	Centro	21.2028	42.1250	51	100	23.4	5.00
Maricá	M. Ribeiro	22.9014	42.5833	39	76	25.6	6.58
	M. Ribeiro	22.9014	42.5833	34	66	23.4	7.58
Miguel Pereira	Centro	22.4667	43.4667	36	74	16.1	6.76
Miracema	P. Tobias	21.4306	42.1044	48	100	20.5	5.00
Resende	Centro	22.4833	44.4333	19	50	33.0	7.00
Rio Bonito	B. Esperança	22.7931	42.5372	55	108	33.0	4.63
S.Seb.do Alto	V.BarroCentro	21.8211	42.0922	54	106	8.0	4.70
	V.BarroCentro	21.8242	42.0983	27	52	19.0	3.85
Sapucaia	Aparecida	22.0322	42.7950	40	78	14.0	6.41
	Jamapara P3	21.8953	42.7086	38	74	34.0	6.76
	Jamapara P4	21.8947	42.7106	41	80	46.0	6.25
Mean	–	–	–	40	82	23.1	5.99

N_T is total number of temperature measurements, Z the depth of the borehole, Γ the temperature gradient and σ is the estimated error in Γ.

low to normal (in the range of 30–70 mW/m^2) in most part the Precambrian fold belts in the state of Rio de Janeiro. Nearly the same range of values is also found in areas of Phanerozoic sedimentary cover. On the other hand, higher than normal heat flow (in the range of 80–100 mW/m^2) have been found for the east-west trending belt of alkaline intrusions of Tertiary age. Additional data from deeper boreholes are necessary in confirming the existence of this thermal anomaly in the southeastern coastal area of Brazil. There are, however, some supporting evidences. Estimates based on geochemical thermometric data indicate that the heat flow is higher than normal in areas of mineral springs, occurring within or close to the belt of alkaline intrusions (Hurter, 1986). Results of ground and air-borne geophysical surveys of the magnetic field reveal several major east west trending magnetic anomalies in this area. Dos Anjos and Vasconcellos (2000) have interpreted these as arising from the emplacement of a large number of mafic dikes of Tertiary age at shallow depths in the crust. Results of magnetotelluric soundings (Machado et al., 2001) indicate the presence of a zone of low electrical resistivity in the area of Silva Jardim, located within the belt of alkaline intrusions. The thermal and tectonic

significance of these observations has recently been examined as part of a separate work (Gomes and Hamza, 2004).

The spatial variations in geothermal regime are best seen in regional maps of the heat flow field. In the present case, numerical representation of the regional heat flow field was attempted making use of commonly available mapping packages such as GMT (Wessel and Smith, 1992) and SURFER (Golden Software Inc., 2002). In such representations, it is standard practice to make use of observed data in setting up a regularly spaced grid of interpolated values. Automatic contouring techniques are subsequently employed in generating the numerical surfaces of heat flow. As an illustrative example, we present in Fig. 2c the regional heat flow map of the state of Rio de Janeiro. The map reveals that heat flow is low to normal in most part of the study area where the basement rocks are metamorphic fold belts of Precambrian age. As mentioned earlier, heat flow appears to be higher than normal in some isolated localities, situated along the east-west trending belt of alkaline intrusions of Tertiary age. These intrusions are believed to be associated with the passage of Trindade mantle plume (Hertz, 1977; Hamza, 1982b). Geothermal data from deep boreholes

Table 2c
Mean thermal conductivity values for the main rock types in the southeastern coastal area of Brazil

Rock type	Thermal conductivity (W/(m K))		
	N	Mean	σ
Fluvial sediments	9	2.7	0.8
Siltstone	3	2.7	1.3
Medium grained sandstone	12	2.8	0.8
Argillaceous sandstone	12	2.2	0.8
Amphibolites	3	3.3	1.6
Quartzite	3	3.1	1.0
Biotitic gneiss	18	3.5	2.0
Banded gneiss	9	3.0	2.0
Facoidal gneiss	12	4.3	2.4
Granite gneiss	3	3.1	2.1
leucocratic gneiss	3	2.8	1.2
Mesocratic gneiss	3	3.9	1.0
Granada-gneiss	12	4.4	3.0
Granite	9	3.1	1.3
Granite-undifferentiated	3	2.7	1.5
Porphyritic granite	12	2.6	0.7
Granitoide	3	3.0	1.7
Tonalitic granitoide	9	3.1	1.3
Granulite	24	3.3	1.7
Metamorphic calc-silicate	9	2.4	1.0
Diabase	3	2.6	0.7

N is number of measurements and σ is the standard deviation.

are necessary to assess the anomalous thermal fields along this belt.

2.2. Central parts of the Brazilian highlands

Brazilian highlands form the central core of the tectonically stable South American Platform area. It includes parts of Arquean cratonic areas in the east and metamorphic fold belts of Proterozoic age in the west. Vitorello et al. (1980) reported heat flow for five localities in the states of Goiás and Tocantins. The values are in the range of 50–70 mW/m^2, which are considered as representative of regional heat flow in the central parts of the Brazilian highlands. However, several large belts of overthrust tectonics occur in this region (Dardenne, 2000; Pimentel et al., 2000) and there are indications that the thermal fields of such terrain are different from that of the surrounding regions. For example, in the Caldas Novas area, metamorphic rocks of the Araxá Group have been thrust over younger rocks of the Bambuí Group, leading to formation of plateaus and uplifted terrains. According to currently accepted regional geologic models, Serra de Caldas plateau constitute an uplifted window of underlying rocks. Upwelling of deep fluids circulating through the under-thrust formations of the Bambui Group are considered as responsible for the widespread occurrence

of thermal springs in this area (Anjos and Veneziani, 1977).

Attempts to carry out temperature logs in this area were not successful because of the presence of submersible pumping equipments in the interior of most of the wells. The availability of geothermal data was thus restricted to measurements of temperatures carried out during pumping tests of wells. Santos et al. (1986) pointed out that such data may be used for calculating thermal gradients, for cases where the extraction of fluids is confined to a single confined aquifer. A brief summary of this method, designated here as the *aquifer temperature method* (AQT), is given in the Appendix. Essentially, the measured wellhead temperatures are corrected using an appropriate model to account for the radial heat loss that occurs during up-flow of fluids. The correction allows determination of the in situ temperature of the aquifer. Santos et al. (1986) made a comparative analysis of the results by conventional, BHT and AQT methods and concluded that differences in gradient values are less than 5%, for the wells considered in the Paraná basin. In the present case, an independent check on the reliability of AQT method has been attempted by comparing measured temperatures in wells under artesian flow conditions with those calculated following the procedure of Santos et al. (1986). The wells are located in the adjacent region of Cachoeira Dourada, to the south of Caldas Novas. As an illustrative example, we present in Fig. 3a the vertical distributions of temperatures for three deep wells (CD-3, CD-5 and CD-7) which present artesian flows. Also presented in this figure are results of temperature log of a shallow bore hole (CD-8) in which no flow occurs. The experimentally determined values of aquifer temperatures and gradient values are given in Table 3a along with calculated values, following the procedures outlined in the Appendix. In this case, errors in aquifer temperatures by the AQT method are found to be less than 1% while those for gradients are less than 2%.

Campos and Costa (1980) reported results of hydrogeological studies of the Caldas Novas area, including temperature and flow rate data for 25 boreholes. The aquifer temperatures were calculated based on the AQT method, the details of which are presented in Table 3b. The vertical distribution of aquifer temperatures is illustrated in Fig. 3b. The results of gradient calculations, presented in the last column of Table 3b indicate values higher than 20 $^{\circ}$C/km for all but two of the boreholes. These results are considered as an indication that the thermal gradients of over-thrust terrain are significantly higher than those for the Precambrian metamorphic fold belts in central Brazil.

Table 2d
Summary of heat flow data for the southeastern coastal area of Brazil

Locality	N	Coordinates		Γ (°C/km)	λ (W/(m K))	q (mW/m^2)
		West longitude	South latitude			
Areas of Precambrian fold belts						
Cambuci	1	−41.9197	−21.4667	33.8	2.7	74 ± 31
Cordeiro	1	−42.3689	−22.0169	19.8	3.1	61 ± 26
Duas Barras	4	−42.5203	−22.0486	15.3	3.1	48 ± 23
Cel, Teixeira	1	−41.9197	−21.4672	19.0	2.7	57 ± 38
Jaguarembé	1	−41.9667	−21.7133	17.2	2.7	46 ± 35
Itatiaia	1	−44.5833	−22.5000	16.5	2.7	45 ± 15
Laje de Muriaé	1	−42.1250	−21.2028	23.4	3.1	70 ± 29
Maricá	3	−42.7519	−22.9014	20.2	2.7	54 ± 29
Miguel Pereira	1	−43.4667	−22.4667	16.1	3.4	50 ± 23
Miracema	2	−42.2000	−21.4167	20.4	2.8	61 ± 31
Niterói	3	−43.0672	−22.9333	40.0	2.7	44 ± 18
Rio Claro	1	−44.0333	−22.4167	55.2	2.4	49 ± 19
Paraíba do Sul	2	−43.3167	−22.1500	17.6	2.8	53 ± 26
Porciúncula	1	−41.9094	−20.8211	13.3	3.4	39 ± 16
Sapucaia	1	−42.7950	−22.0333	14.2	3.4	49 ± 30
Teresópolis	3	−42.9444	−22.4333	20.0	3.1	65 ± 26
Valão de Barro	3	−42.0922	−21.8211	9.4	4.4	30 ± 19
Vassouras	1	−43.5333	−22.3500	14.1	2.7	55 ± 14
Mean	–	–	–	18.1	3.1	53 ± 11
Areas with phanerozoic sedimentary cover						
Baixa Grande	1	−41.1333	−21.9578	18.6	3.2	50 ± 19
Boa Vista	1	−41.1033	−22.0167	26.4	2.7	71 ± 21
Coronel Josino	1	−41.3417	−21.5000	21.3	3.1	58 ± 19
Horto	1	−41.2864	−21.7636	18.7	2.8	56 ± 15
Saquarema	1	−42.5167	−22.8500	15.4	2.7	42 ± 12
São Sebastião	1	−41.2111	−21.8539	35.3	3.7	78 ± 31
Volta Redonda	1	−44.2000	−22.5667	20.3	2.7	57 ± 31
Mean	–	–	–	20.1	2.9	59 ± 10
Areas within the belt of alkaline magmatism of Tertiary age						
Angra dos Reis	2	−44.2833	−23.0333	46.2	2.7	100 ± 35
Carapebus	1	−41.6656	−22.1869	30.2	2.7	82 ± 25
Resende	5	−44.7667	−22.7833	40.0	2.7	80 ± 32
Rio Bonito	1	−42.5372	−22.7931	32.8	2.7	89 ± 27
Mean	–	–	–	40.7	2.7	88 ± 10

N is the number of boreholes, Γ the mean temperature gradient, λ the mean thermal conductivity and q is the representative value of local heat flow density.

Table 3a
Comparison of observed values of aquifer temperatures and thermal gradients with those calculated using the AQT method, for artesian wells in Cachoeira Dourada, Central Brazil.

Well	Depth (m)	Flow Rate (m^3/h)	Temperature (°C)		Gradient (°C/km)	
			Observed	Calculated	Observed	Calculated
CD-3	320	20	37.55	37.34	43.71	43.04
CD-5	320	15	37.73	37.82	44.29	44.58
CD-7	380	60	37.12	37.04	42.32	42.09
CD-8	92	0	–	35.8[a]	–	–

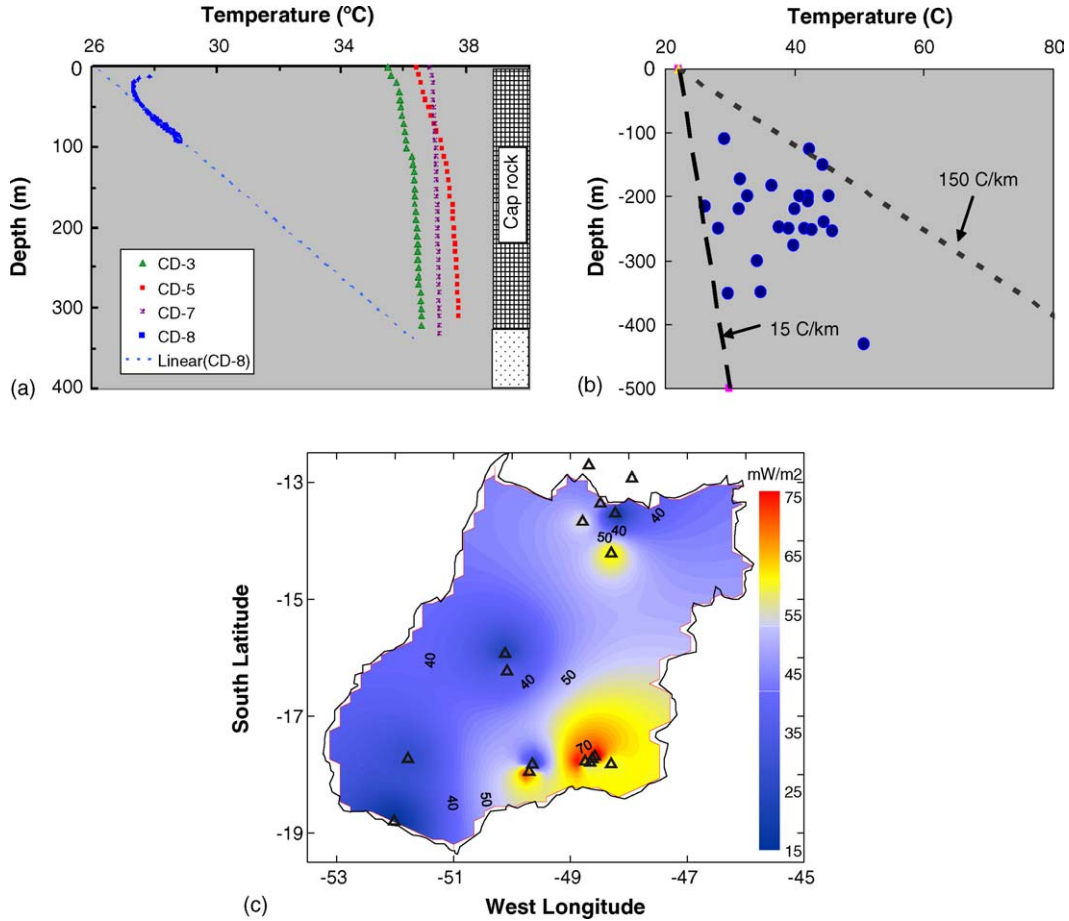[a] Extrapolation based on least square fit.

Fig. 3. (a) Results of temperature logs in four wells in Cachoeira Dourada, state of Goiás (Central Brazil). CD-3, CD-5 and CD-7 are artesian wells with natural flows. CD-8 is a shallow well in which no flow occurs. The dashed line refers to extrapolation based on least square gradient for the linear segment in well CD-8. A simplified lithologic sequence is indicated on the right side, consisting of basalt (cap rock) and sandstone (aquifer). (b) Temperatures measured in deep wells in the Caldas Novas area, in the state of Goiás (Brazil). The dashed line refers to the mean gradient of 15 °C/km reported by Vitorello et al. (1980). The dotted line refers to a gradient of 150 °C/km. (c) Preliminary heat flow map of the state of Goiás, Central Brazil. The triangles indicate locations of heat flow measurements. The numbers on the side bar refer to heat flow values in mW/m^2.

The rock types in this region are mainly schists (sericite, muscovite and biotite) and quartzites of the Precambrian Araxá Group. Locally present are calc schists, metamorphic calcites, marble, graphitic, chlorite and granada schists, schists with aluminum-silicate amphiboles, gneisses and metabasites. Metarenites of the Bambuí Group, which are younger in the local stratigraphic sequence, are present in the Serra de Caldas plateau. Representative values of thermal conductivity are available only for a limited number of this relatively large set of rock types. Vitorello et al. (1980) reported thermal conductivity values for seven rock types occurring in eleven localities. More recently, Ferreira (2003) estimated thermal conductivity from mineral compositions of rocks occurring in five additional localities. Analysis of these data sets reveals sys-

tematic variations in thermal conductivity, associated mainly with the lithological characteristics. For example, rocks of mafic and ultramafic composition are found to have thermal conductivity in the range of 2–3 W/(m K) while quartzites seem to be characterized by values in the range of 4–7 W/(m K). Intermediate values in the range of 2.5–4 W/(m K) are found for schist and gneisses.

Heat flow values were calculated as the product of apparent temperature gradients and the harmonic mean thermal conductivity of the main rock types encountered in boreholes. The results, presented in column six of Table 3c, indicate that local heat flow in the Caldas Novas region is higher than normal, with values in excess of 150 mW/m^2. Supporting evidences, pointing to the existence of anomalous geothermal fields in the over-thrust

Table 3b
Summary of temperatures, flow rates and calculated gradients by the AQT method for the area of Caldas Novas, Goiás (Central Brazil)

Identification number	Depth (m)	Outflow temperature (°C)	Flow rate (m³/h)	Aquifer temperature (°C)	Temperature gradient (°C/km)
191	150.0	44.0	45.0	44.3	142.0
192	200.0	42.0	90.0	42.2	96.0
193	125.0	42.0	40.0	42.3	154.4
194	220.0	39.0	20.0	40.0	77.3
195	248.0	37.0	26.0	37.7	59.3
196	208.0	41.7	40.0	42.2	92.3
197	172.0	29.0	2.3	31.7	50.6
198	220.0	31.0	20.0	31.4	38.2
199	200.0	40.3	34.0	40.9	89.5
200	200.0	29.0	2.0	32.8	49.0
201	250.0	38.0	6.0	41.6	74.4
202	350.0	31.0	4.5	34.8	33.7
203	300.0	33.0	13.0	34.3	37.7
204	276.0	38.0	13.0	39.8	60.9
206	250.0	28.2	60.0	28.3	21.2
208	183.0	36.0	24.0	36.5	73.8
209	252.0	42.0	44.0	42.6	77.8
210	430.0	48.6	27.4	50.8	64.7
211	110.0	29.0	30.0	29.1	55.5
212	352.0	28.3	0.75	29.8	19.3
214	249.0	38.8	67.0	39.1	64.7
215	254.0	30.8	1.0	45.8	89.8
218	215.0	26.0	24.0	26.1	14.4
219	200.0	44.5	24.0	45.4	112.0
220	240.0	44.4	118.0	44.6	90.0

terrain of Brazilian highlands, may also be found in estimates of heat flow by geochemical methods. Preliminary chemical analyses of thermal waters from the Caldas Novas region were carried out by Campos and Costa (1980). More recently, geochemical characteristics of the thermal springs in the central parts of the Brazilian highlands were investigated as part of a joint Brazilian–Italian geothermal project (Calvi et al., 2000). Ferreira (2003) used the data gathered in this latter work along with those reported in earlier investigations in obtaining estimates of heat flow by the geochemical method. The results are given in Table 3c.

A preliminary heat flow map of the state of Goiás is presented in Fig. 3c, based on data presented in Table 3. The prominent features in this map are the heat flow anomalies in southern (Caldas Novas) and northern (Minaçu) parts of the state of Goiás. The lateral extension of these heat flow areas are poorly defined, as suitable data are not available for the neighboring regions.

2.3. Paraná basin

This is an intra-cratonic sedimentary basin in the southwestern parts of the Brazilian platform, which cov-

Table 3c
Summary of heat flow data by the AQT method for the area of Caldas Novas, Goiás (Central Brazil)

Locality	Coordinates		Γ (°C/km)	Λ (W/(m K))	q (mW/m²)
	Latitude	Longitude			
Rio Quente (5)	48.7475	17.7765	>100	3.5	350 ± 100
Pirapetinga (4)	48.5810	17.6904	76–100	2.7	250 ± 75
Caldas Novas (22)	48.6251	17.7361	42–109	2.7	200 ± 75
Tucum (2)	49.6500	17.8250	18.0	3.0	54 ± 30
Bagre (2)	49.7040	17.9500	81.0	3.0	240 ± 80
Area 103 (1)	48.3030	17.8230	57.9	2.7	180 ± 80

The numbers in brackets refer to wells with temperature measurements. Γ is the temperature gradient, Λ the thermal conductivity and q is the heat flow density (adapted from Ferreira, 2003).

Table 3d
Estimates of heat flow by geochemical methods for the Caldas Novas area

Locality	Coordinates		Temperature (°C)		Heat flow (mW/m^2)
	Longitude	Latitude	Outflow	Reservoir	
Rio Quente (>30)	−48.7475	−17.7765	32–42	66	65
L. Pirapetinga (>10)	−48.5810	−17.6904	32–49	80	86
Serra de Caldas (1)	−48.6628	−17.7939	24.6	34	19
Caldas Novas (>30)	−48.6251	−17.7361	44–56	88	97
Formoso (1)	−48.7911	−13.6749	33.1	80	85
Faz. Paranã (>5)	−47.9467	−12.9338	26.1–37.0	60	56
Jaú Tocantins (>5)	−48.6848	−12.7188	26.7–39.2	67	67
Minaçu (>5)	−48.4851	−13.3619	29.0–41.2	71	73
Novo Accordo (>5)	−47.4849	−10.0374	29.0–31.9	47	37

The numbers in brackets refer to springs in each locality (adapted from Ferreira, 2003).

ers an area of over 1.6 million square kilometers in southern Brazil. It also extends into Uruguay and Argentina in the south and to Paraguay in the west. Eston et al. (1983) carried out a detailed study of geothermal field in the southwestern region of Brazil, as part of an exploration project for evaluation of the thermal maturation of hydrocarbons in the Paraná basin. In this work, thermal gradient values were determined for 81 localities, of which 27 are based on results of conventional methods while the remaining 54 were calculated using bottom-hole temperatures (BHT) measured in deep oil wells. The details of data obtained by conventional methods have already been discussed in the previous works of Vitorello et al. (1980), Santos et al. (1986) and Hamza and Muñoz (1996). The gradient and heat flow values obtained using BHT methods are discussed in the work of Eston et al. (1983).

The bottom-hole temperature data need to be corrected for the disturbing effects of drilling disturbances. Procedures for such corrections have already been discussed extensively in the literature (see, for example, Ribeiro and Hamza, 1986). The correction procedure adopted by Eston et al. (1983) are based on the assumption that perturbations by drilling activity may be represented as a line source of heat (see, for example, Lachenbruch and Brewer, 1959). This is essentially the standard 'Horner type' (Horner, 1951) correction. In some cases, where adequate data were available, corrections were also made using the models proposed by Middleton (1979) and Leblanc et al. (1980). A comparison of these model results, is presented in Fig. 4a, for a limited data set from the Paraná basin. It indicates that the overall effect of corrections is a small increase in the gradient values, often less than 10% of the uncorrected value. In particular, the gradient values after correction by the circular well model (Leblanc et al., 1980) are

found to be not significantly different from the uncorrected ones. On the other hand, the line source model leads to corrections of the order of 10%.

The vertical distribution of the corrected bottom-hole temperatures is presented in Fig. 4b. Least square fit to this data set indicates an overall gradient value of 19.7 ± 1.1 °C/km, about 8% higher than the uncorrected value of 18.4 °C/km. In a later study, Hurter (1992) reported BHT values for 64 wells, the basic data set being in large part the same as that employed in the earlier work by Eston et al. (1983). Hurter (1992), applied the empirical AAPG correction procedure (see Appendix A) and obtained an overall gradient value of 22.4 °C/km. In the present work, we have retained the values obtained by Eston et al. (1983), as these are based on the relatively more reliable and non-empirical correction procedures.

Eston et al. (1983) also reported results of thermal conductivity measurements on 1083 core samples and determined representative thermal conductivity values of the main rock types and sedimentary formations of the Paraná basin. A summary of the final results is given in Table 4a along with the data reported in the later study by Hurter (1992). The gradient and thermal conductivity data were used in determining heat flow for 64 localities. The set of heat flow data in Tables 4b–4d refer, respectively, to the southern, western and northern parts of the Paraná basin. The regional heat flow map of Paraná basin, presented in Fig. 4c, is based on the data in Table 4. This map indicates that heat flow is low to normal (<60 mW/m^2) in the central parts of the Paraná basin, but relatively high (>60 mW/m^2) along its northern and eastern borders. The region of high heat flow on the northeastern parts of the basin is in fact the southward extension of the geothermal anomaly of the region of Caldas Novas, discussed in Section 2.2.

Table 4a
Summary of thermal conductivity data for the Paraná basin

Formation	Eston et al. (1983)			Hurter (1992)		
	N	λ (W/(m K))	σ (W/(m K))	N	λ (W/(m K))	σ (W/(m K))
Quaternary	6	2.26	0.16			
Bauru	64	3.7	0.33			
Serra Geral	473	1.81	0.31	7	1.86	0.10
Botucatu	226	4.04	0.77	5	2.76	0.29
Piramboia	10	2.71	0.32			
Rio do Rasto	53	2.37	0.46	34	2.27	0.09
Teresina	28	2.27	0.22	11	2.04	0.14
Estrada Nova	19	1.77	0.32			
Serra Alta	8	1.9	0.17	27	2.33	0.12
Irati	43	2.34	0.34	10	2.20	0.34
Palermo	18	2.93	0.3	12	2.62	0.38
Tatui	9	1.76	0.36			
Rio Bonito	24	2.60	0.36	30	2.87	0.16
Itararé	93	2.78	0.55	78	3.37	0.12
Ponta Grossa				12	2.57	0.26
Furnas						
Basement	9	3.84	0.89			
Total	1083			226		

N is the number of samples, λ the mean thermal conductivity and σ is the standard error of the mean.

Table 4b
Heat flow values by BHT method for localities in the southern parts of the Paraná basin, in the states of Rio Grande do Sul and Santa Catarina

| Locality/well	Coordinates		Depth (m)	Heat flow (mW/m^2)	
	Latitude	Longitude		Eston et al. (1983)	Hurter (1992)
AL1RS	−55.7700	−28.8200	2044	42	42
Abelardo Luz	−52.3280	−26.5650	3881	51	42
Atanasio	−51.6644	−28.7014	2251	51	51
Barra Nova	−49.7569	−27.5089	1101	76	
Caçador	−51.0150	−26.7750	1935	72	68
Canoinhas	−50.5203	−26.3019	1776	69	70
Esmeralda	−51.1900	−28.0540	2424	49	
HV1SC	−51.4600	−27.2200	2700	60	60
Itacurubi	−54.9917	−29.0167	2576	52	44
Lages	−50.3261	−27.8167	1334	82	
MA1RS	−51.6600	−27.5900	2715	58	58
Matos Costa	−51.1480	−26.4730	1967	60	58
MR1RS	−51.9300	−27.5300	2589	61	61
Muitos Capões	−51.1820	−28.3140	2312	61	
PA1SC	−49.7400	−27.6000	1126	74	74
Piratuba	−51.7794	−27.4242	2271	58	53
Porto União	−51.0569	−26.2739	2327	61	60
RCH1SC	−52.0400	−26.6600	3273	54	54
Ronda Alta	−52.7558	−27.9111	3418	38	39
S.Luiz Gonzaga	−54.9608	−28.4083	2401	44	44
Seará	−52.3110	−27.1490	3828	55	
Taquará Verde	−51.3158	−26.7436	2237	58	
TG1SC	−51.2500	−27.0800	2431	69	69
Torres	−49.8000	−29.3300	990	71	71
Tres Pinheiros	−51.4336	−26.7131	2998	41	41
TVSc	−51.3200	−26.7400	2235	51	51
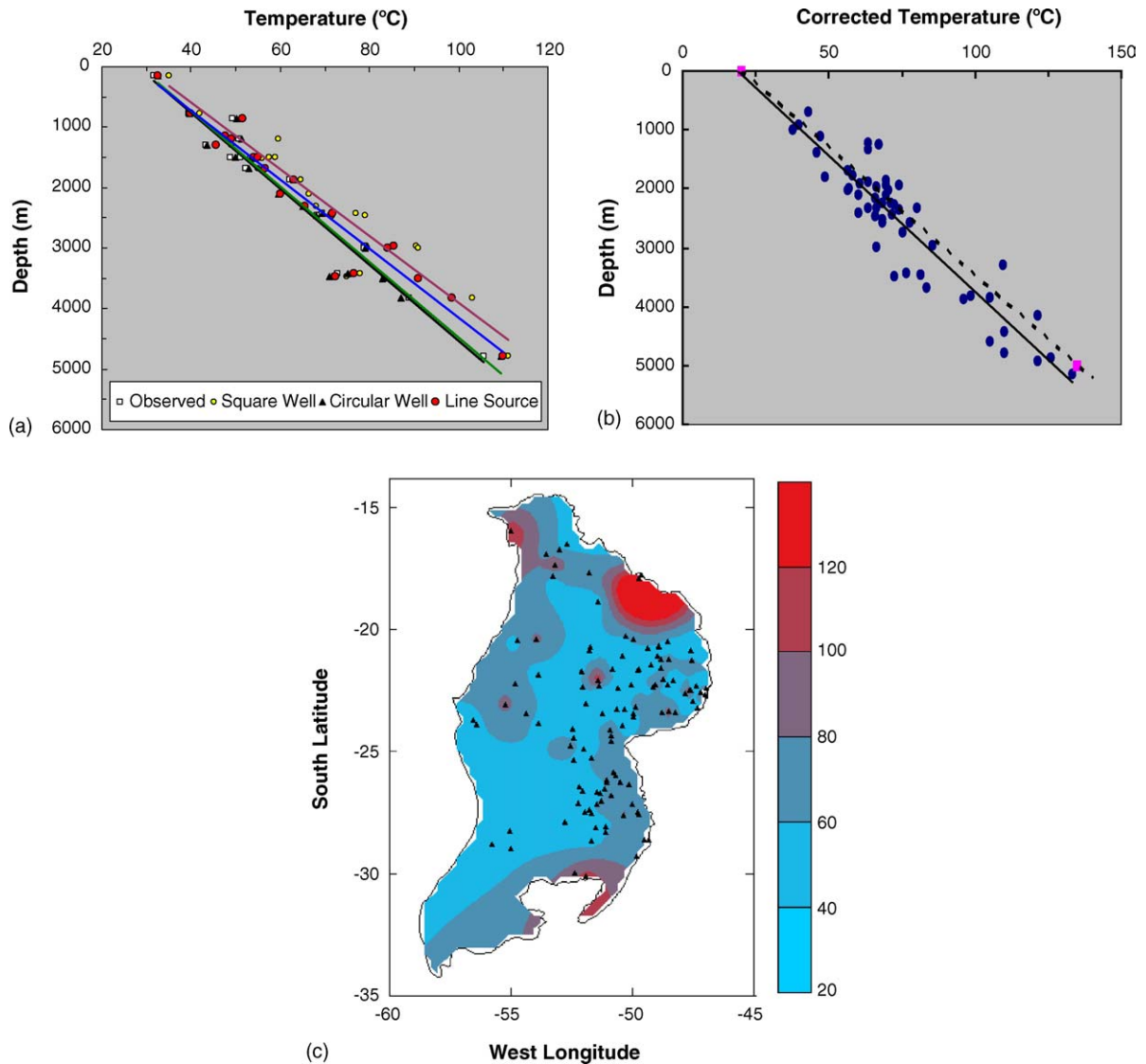
Fig. 4. (a) Comparative analysis of observed and corrected BHT values. See text for details of models used for corrections. (b) Temperatures corrected for drilling disturbances in deep wells in the Paraná basin. The least square fit, indicated by the dashed line, gives an overall gradient of 20.1 °C/km. The dotted line refers to the gradient value of 22.4 °C/km for the empirical AAPG correction. (c) Heat flow map of the Paraná basin in southern Brazil. The triangles indicate locations of heat flow measurements. The numbers on the side bar refer to heat flow values in mW/m^2.

2.4. Central Andean region of northern Chile and southern Bolivia

Since the pioneering works by Uyeda et al. (1978) and Watanabe et al. (1980) only some isolated efforts has been carried out for measuring heat flow in the central Andean region. Henry and Pollack (1988) reported results of heat flow measurements for 29 localities, comprising northern parts of Chile and southern parts of Bolivia and Peru. Following this, Muñoz and Hamza (1993) reported results of temperature logs for four boreholes in the central part of Chile and one in its northern part. They also presented results of thermal conductivity measurements on 39 core samples representative of the main rock types encountered in these bore holes. Heat flow values calculated for these five sites are given in Table 5a.

More recently, Springer and Foerster (1998) reported results of heat flow measurements for 29 localities in the Central Andean Zone. Both conventional and BHT methods were used. Their data set includes new values of heat flow for sixteen sites in Bolivia and five sites in Chile. In addition, Springer and Foerster (1998) reexamined the results of earlier measurements by Uyeda et

Table 4c
Heat flow values by the BHT method for localities in the central and western parts of the Paraná basin, in the states of Paraná and Mato Grosso do Sul

Locality/well	Coordinates		Depth (m)	Heat flow (mW/m^2)	
	Latitude	Longitude		Eston et al. (1983)	Hurter (1992)
Altonia	−53.9020	−23.8740	4933	54	
AP1PR	−51.2200	−23.4900	4300	42	42
AV1PR	−51.9100	−23.0900	2787	58	58
Campo Grande	−54.7192	−20.4858	2524	54.8	53
Cândido Abreu	−52.4239	−24.4928	1888	60	61
Chapeu do Sol	−52.3070	−22.9600	2465	42	
CM1PR	−52.4300	−24.1100	4455	46	46
Dourados	−54.8128	−22.2681	4161	72.7	59
GP1PR	−51.6600	−25.3100	3650	62	62
J1PR	−49.8700	−23.2200	2684	69	69
LS1PR	−52.4200	−25.4100	3968	54	54
LV1PR	−51.5000	−28.1700	2362	41	
Mallet	−50.7861	−25.8778	1862	81.2	
Monjolinho	−50.8706	−24.3744	2018	59.7	58
Ortigueira	−50.9500	−24.2083	2025	82	73
Quatiguá	−49.9136	−23.5667	1385	55	55
RC1PR	−50.7000	−26.0100	1999	70	70
Reserva	−50.8833	−24.6250	1910	65	53
Rio Aporé	−51.4000	−18.9000	3476	46.1	39
Rio Ivai	−50.8590	−25.0110	5337	68.8	
Rio Piqueri	−53.4400	−24.0103	4863	76.2	
S. J. da Serra	−50.7411	−23.7275	2346	64	64
União de Vitória	−51.0333	−26.1917	2162	65.4	64

al. (1978) and Henry and Pollack (1988) and presented revised values of heat flow for eight additional sites.

A poorly represented region in these investigations is the Southern Cordillera of Peru. This is an area of subduction related magmatism, as evidenced by widespread occurrence of shallow seismicity and recent volcanic activity. Steinmuller (2001) reported geothermal data on hot springs located at twelve sites within this area, which included also estimates of reservoir temperatures. These data has been used in estimating heat flow based on the geochemical method. The results, presented in Table 5b, indicate heat flow values in excess of 100 mW/m^2, significantly higher than the values in the range of 40–90 mW/m^2 reported in the earlier measurements in southern Peru by Henry and Pollack (1988). New temperature measurements in deep boreholes are necessary to assess the nature of deep crustal heat flow in this area.

Springer and Foerster (1998) and Springer (1999) considered their results as indicative of a broad region of relatively high heat flow (>90 mW/m^2) in Central Andes and presented a regional heat flow map of this region. In view of the availability of new heat flow estimates for the cordilleras of Southern Peru, a revised heat flow map of this region, was prepared (Fig. 5). It reveals an arc shaped region with heat flow greater than 100 mW/m^2 between south latitudes of 15 and 30. The coastal region in northern Chile to the west and the Precordilleran basins to the east are found to have relatively low heat flow (<60 mW/m^2). The tectonic implications
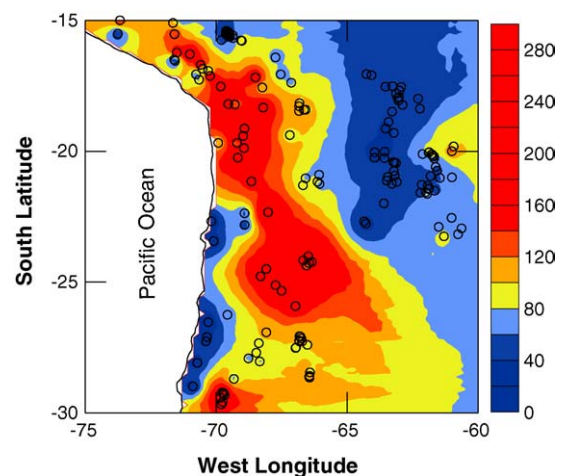

Fig. 5. Revised Heat flow map of Central Andean Region, including the southern volcanic cordillera of Peru. The circles indicate locations of heat flow measurements. The numbers on the side bar refer to heat flow values in mW/m^2.

Table 4d
Heat flow values by the BHT method for localities in the eastern and northern parts of the Paraná basin, in the states of São Paulo, Mato Grosso and Goiás

Locality/well	Coordinates		Depth (m)	Heat flow (mW/m²)	
	Latitude	Longitude		Eston et al. (1983)	Hurter (1992)
Amadeu Amaral	−50.0417	−22.3022	2966	56.3	50
Alto Garças	−53.5333	−16.9167	1946	72.8	79
Amambai	−55.2417	−23.1000	3293	85.8	
Aracatuba	−50.4158	−21.1000	2731	51.7	
AS1SP	−47.5800	−22.5200	1335	66	66
AT1SP	−47.8100	−22.6700	1262	56	56
CP1SP	−48.5100	−23.3800	1545	99	
Cuiabá Paulista	−52.0486	−22.4000	5136	54.1	48
Guarei (GU−3−SP)	−48.2292	−23.4167	982	62.9	54
Jatai	−51.7806	−17.7317	2106	72.4	68
Lagoa Azul	−50.8300	−21.3500	4416	54.1	
Lins	−49.7561	−21.6922	3460	49.8	44
Olimpia	−48.9278	−20.6875	2568	59.1	53
Paraguaçu Paulista	−50.6047	−22.4153	3664	44	42
Paranapanema	−48.7744	−23.4353	1684	69	63
Piratininga	−49.1522	−22.3839	2104	55.6	54
Pitanga	−47.6403	−22.5444	1229	119.6	
Pres. Epitácio	−52.1019	−21.7583	3851	50.7	47
RP1MT	−53.9500	−20.4200	3366	87	87
SD1MT	−53.8700	−21.8800	3003	51	51
Taciba	−51.3414	−22.3333	4783	48.9	43
TQ1MT	−53.2600	−17.8700	2021	54	54
Três Lagoas	−51.6783	−20.7500	4583	46	46

Table 5a
Heat flow values for five sites in Northern Chile, based on data reported by Muñoz and Hamza (1993)

Locality	Coordinates		Heat flow (mW/m²)	
	Longitude	Latitude	Mean	σ
Pehuen	−73.5456	−37.6522	63	9
Lebu	−73.6331	−37.6403	172	23
Dolores	−69.9167	−19.6833	93	15
Curanilahue	−73.5000	−37.4167	79	12
Cholchol	−72.8333	−38.5833	89	11

Table 5b
Estimates of heat flow for nine sites in the Southern Cordillera of Peru, based on geochemical data by Steinmuller (2001)

Locality	Coordinates		Temperature (°C)			Heat flow (mW/m²)
	Longitude	Latitude	Surface	Outflow	Reservoir	
Puquio	−74.0000	−14.5000	15	69	120	154
Parinacochas	−73.6666	−15.0000	15	81	105	132
Cailloma	−71.6470	−15.1000	15	57	90	110
Chivay	−71.5900	−15.5290	15	84	115	147
Chachani	−71.5000	−16.2350	15	34	145	191
Ubinas	−71.0000	−16.2940	15	76	175	235
Calacoa	−70.5880	−16.7050	15	89	165	221
Tutupaca	−70.2350	−17.1200	15	88	170	228
Trio Maure	−69.8230	−17.5290	15	87	130	169

of this high heat flow zone are not well understood, as magma activity in this region is restricted to a narrow well-defined north-south trending arc-shaped belt. High regional heat flow would normally imply existence of either widespread occurrence of heat sources at shallow levels in the crust or a significant thermal anomaly in deeper parts of the subcrustal lithosphere. Improvements in geothermal measurements that can determine more accurately the lateral and vertical distribution of local thermal fields are necessary to elucidate the relation between heat flow and magma activity in this region.

2.5. Copahue area in Western Argentina

This area is situated in the Neuquén province at the western border of Argentina with Chile. The structural setting of this region is marked by large fracture systems associated with subduction related magmatic activity and tectonic processes operating on the southern part of the Andean zone. Mas et al. (2000) report results of geothermal studies carried out as part of geothermal energy exploration programs. Determination of geothermal gradients and heat flow have been carried out in 12 shallow wells. Most of the gradient values encountered are in the range of 50–250 °C/km, substantially higher than the gradients reported for the eastern part of the Patagonian platform (Robles, 1988). The estimated heat flow values are in the range of 46–426 mW/m^2, giving an overall mean value of 163 mW/m^2. Lateral extension of this heat flow anomaly is poorly defined, as suitable measurements have not so far been carried out in the neighboring areas.

2.6. Chaco plains of Paraguay

Chaco Plains is part of a large system of foreland basins, limited by Andean ranges in the west and the Brazilian Shield in the east. Within Paraguay, the Chaco Plains is composed of several depo-centers in the west (Carandaity, Curupaity and Pirity sub-basins) and in the east (the San Pedro Low and Pilar sub-basins), separated by the Central Chaco Uplift. The Chaco Plains merges with the Santa Cruz-Tarija province to the west, Paraná basin to the east and the Pampas basin to the south. According to Zalan (1987), the subsidence phases of Chaco and Paraná basins were initiated during the Brasiliano folding event that affected large sectors in the central part of the South American platform. Geologic correlation studies (see, for example França et al., 1995) reveal that the rock formations of the Chaco basin form a contiguous system of sedimentary sequences that span onto the adjacent basins of Paraná and Santa Cruz. The differences in stratigraphic sequences are restricted to the initial basal deposits and younger depositional sequences of Eocene and Quaternary age.

Kuhn (1991) reported bottom-hole temperatures and gradient values for 36 deep wells drilled for oil exploration in the Chaco Plains. The wells are located mainly in the sub-basins of Carandaity, Curupaity and Pirity and in the area of Central Chaco Uplift. In a more recent work on geologic evolution of Chaco Plains, Wiens (1995) also reproduced temperatures and gradient values for the same group of wells. These data are presented in Table 6a along with estimates of gradient values. Least square fits to ensembles of uncorrected BHT data sets indicate temperature gradients of 24.4 ± 2.1 °C/km for the Carandaity sub-basin, 39.9 ± 10.1 °C/km for the Piriity sub-basin and 40.8 ± 4.3 °C/km for the area of Central Uplift.

Information on drilling history and circulation times of drilling fluids in these wells are currently not available. Thus, only empirical corrections, based on the depths of BHT measurements have been attempted in the present work. Least square fits to the BHT data sets with AAPG corrections indicate temperature gradients of 28.8 ± 2.1 °C/km for the Carandaity sub-basin, 40.6 ± 10.1 °C/km for the Pirity sub-basin and 44.6 ± 4.3 °C/km for the area of Central Uplift. The AAPG corrections have lead to higher values of gradients, especially for data sets from shallow wells. The corrected values of temperatures and gradients are given in Table 6a. The vertical distribution of corrected temperatures is illustrated in Fig. 6a.

Thermal conductivity data are, at present, available only for sedimentary rock formations that are contiguous with the eastern and western borders of the Chaco Plains. Practical difficulties in obtaining representative samples of deep lying strata, encountered in wells drilled prior to 1980s, makes direct determination of thermal properties a difficult task. Similar problems were also encountered in the earlier works by Henry and Pollack (1988) and Springer and Foerster (1998). A convenient alternative in such cases is to make use of regionally averaged values of thermal conductivity. In this context, we note that Henry (1981) reported thermal conductivity values for rock formations of the Santa Cruz – Tarija Province to the west of Chaco Plains. According to Lindquist (1998) the rock formations of western Chaco Plains and neighboring Santa Cruz – Tarija Province constitute a continuous regional system of sedimentary sequences. In addition, there are considerable affinities in composition and structure of the main rock formations of these sub-basins, as can be seen from the stratigraphic correlation charts and results of seismic reflection

Table 6a
The stratigraphic correlation chart for the western Chaco and the Santa Cruz–Tarija province (Lindquist, 1998) and the corresponding thermal conductivity data (Henry, 1981)

Age	Contiguous formations		Thermal conductivity (W/(m K))
	Western Chaco	Santa Cruz-Tarija	
Tertiary	Chaco Fm	Upper Chaco	3.4
		Yecua	3.1
		Petaca	3.4
Cretaceous	Sta. Barbara	Cajones	2.4
	Palo Santo	–	–
	Basic Magmatism	Basic Magmatism	(1.8–2.0[a])
Jurassic	Berta		–
Triassic		San Diego	–
Permian		Cangapi	3.5
Carboniferous	Palmar de las Islas	San Telmo	4.5
		Escarpment	3.9
		Taiguati	2.8
		Tarija	2.7
		Tupambi	3.0
Siluro-Devonian	San Alfredo, Cerro Leon	Los Monos, San Benito	2.4
Cambro-Ordovician	Itapucumi	Sama, Camacho	–

[a] Calculated from mineral composition data by Comin-Chiaramonti et al. (1996).

profiles (see, for example, Wiens, 1995). Thus, formation thermal conductivity for the Santa Cruz – Tarija Province, reported by Henry (1981), is considered as representative of the corresponding strata in the western part of Chaco Plains. A similar situation exists also for the eastern parts of Chaco Plains that are contiguous with the adjacent Paraná basin. According to Fulfaro (1996), rock formations in these two areas constitute a continuous regional system of sedimentary sequences, with considerable affinities in composition and struc-

ture. Thus, formation thermal conductivity values for the Paraná basin, reported by Eston et al. (1983), is considered as representative of the corresponding strata in the eastern parts of the Chaco Plains. In the present case, the seismically determined thickness of the main rock formations (see, for example, Wiens, 1995) were used in conjunction with the respective formation thermal conductivity values for evaluating the overall thermal resistance of the sedimentary strata at the locations of the wells. The respective stratigraphic correlation charts

Table 6b
The stratigraphic correlation chart for the eastern Chaco and Paraná basins (Wiens, 1995) and the corresponding thermal conductivity data (Eston et al., 1983)

Age	Contiguous Formations		Rock type	Thermal conductivity (W/(m K))
	Eastern Chaco	Paraná		
Tertiary	Tertiary	Tertiary	Sandstone	2.6
Cretaceous	Acaray	Bauru	Sandstone	3.0
	Mafic Magmas	Mafic Magmas	Basalts/diabase	1.8–2.0
Jurassic	Misiones	Botucatu	Sandstone	4.0
Triassic		Piramboia	Sandy Shale	2.8
Permian	Independência	Rio Bonito Passa Dois	Sand and mudstone	2.7
Carboniferous	Cornel Oviedo	Itararé Aquidauana	Shale and mudstone	2.6
Siluro-Devonian	Asu	Ponta Grossa	Marine shales	2.3
		Furnas	Sandstone	3.1
Cambro-Ordovician	Itapucumi	Rio Ivaí	Claystone/conglomerates	2.4

Table 6c
Bottom-hole temperatures (Kuhn, 1991), temperature gradients with AAPG corrections (*G*) and estimated heat flow values (*q*) for the Chaco Plains, Paraguay

Locality	Coordinates		Depth (m)	BHT (°C)	G (°C/km)	q (mW/m²)
	Latitude	Longitude				
Carandaity sub-basin						
Federica	−62.1997	−21.5833	800	40.0	16.6	47
Hortensia	−61.6575	−21.5081	765	41.1	18.9	52
Alicia	−61.8158	−20.9500	1305.4	55.6	22.2	62
Brigida	−61.9228	−21.3138	1512.7	58.9	21.3	60
Christina	−61.8905	−21.4483	643.1	38.3	18.1	50
Dorotea	−62.1500	−21.2833	853.4	44.4	20.8	57
Emilia	−62.1205	−20.1095	1022	51.1	23.9	66
Isabel	−61.4611	−21.0205	944.9	47.2	21.7	60
Julia	−61.6200	−20.6017	1280.1	53.3	20.8	58
Katerina	−61.5638	−20.7417	1139.6	50.6	20.9	56
Olga	−61.8783	−21.4200	1171.3	54.4	23.7	65
Luciana	−61.7200	−20.1779	819.3	45.6	23.0	63
Central uplift						
Mendoza-1	−61.7555	−20.1250	791.8	62.2	44.9	117
Mendoza-2	−61.8700	−20.0388	1246.6	64.4	30.3	82
Mendoza-3	−61.8867	−20.0533	693.4	55.0	40.8	107
Pure.Mendoza	−61.6833	−20.2000	3242.7	157.2	40.2	109
Marta	−61.6742	−20.2750	827.5	44.4	21.5	59
Nola	−61.7868	−20.1303	760.1	43.3	21.9	60
Lagerenza	−61.0000	−20.0000	2889.5	176.7	51.9	138
Cerro Leon	−60.9333	−19.8167	1970.1	98.9	36.6	95
Madrejon	−59.4833	−20.4167	1727.6	107.8	46.9	125
Gato	−58.8750	−20.0583	1646.3	76.7	30.3	83
Toro	−58.9500	−20.1328	3417.7	150.6	36.2	99
Lopez	−59.9667	−21.7667	1730.9	82.2	32.0	84
Parapiti-1	−61.0000	−21.0000	2834.2	117.8	32.1	85
Parapiti-2	−62.0000	−21.5667	2350.9	104.4	33.0	87
Don Quixote	−61.9453	−21.6300	2894.4	122.2	33.0	91
Pirity sub-basin						
Palo Santo	−60.7668	−23.1722	3765.2	132.2	28.0	85
Berta	−61.0105	−22.5467	4792.4	164.4	28.7	76
Anita	−61.5050	−22.8900	4127.9	148.9	29.6	89
Gloria	−60.6333	−22.9487	4015.1	141.1	28.5	76
Carmen	−61.3038	−23.2517	4511	174.4	32.7	89
Nazaret	−59.8600	−22.6550	4025	136.1	27.1	73
San Pedro Low						
Asuncion-1	−56.4167	−23.9170	3223	–	21.1	66
Asuncion-2	−56.5333	−23.7632	2926	–	18.2	59

and thermal conductivity of the main rock types occurring in the western and the eastern parts of the Chaco Plains are presented in Tables 6b and 6c, respectively.

The corrected BHT gradient and estimated thermal conductivity values were used in calculating heat flow for 35 localities in the Chaco Plains (Table 6c). The preliminary heat flow map of Paraguay, based on the data set, is presented in Fig. 6b. This map reveals low to normal heat flow (in the range of 40–70 mW/m²) in the eastern parts and a zone of relatively high heat flow (>80 mW/m²) in the northwestern parts. The westward

and northward extensions of this high heat flow zone are poorly defined, there being no heat flow data in the adjacent region extending to the eastern part of Bolivia.

2.7. Sub-Andean basins of Peru and Ecuador

The sub-Andean region between latitudes 5°N′ and 10°S′ include Putumayo and Oriente basins in the north and Marañon basin to the south. According to Pindell and Tabbutt (1995) these basins are actually depo-centers of the large north-south trending sub-Andean depression in
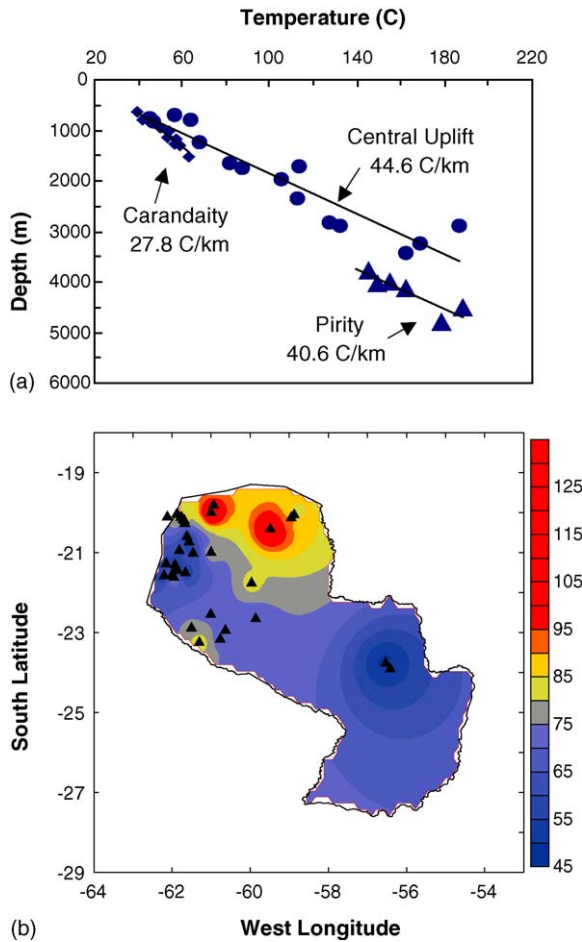
Fig. 6. (a) Bottom-hole temperatures and gradients in the sub-basins of Chaco Plains, Paraguay. The symbols (squares, circles and triangles) indicate, respectively, data from the Carandaity sub-basin, Central uplift and Pirity sub-basin. The lines indicate least square fits to BHT data sets with AAPG corrections. (b) Preliminary heat flow map of Paraguay. The triangles indicate locations of heat flow measurements. The numbers on the side bar refer to heat flow values in mW/m^2.

Table 7a
Thickness of Cretaceous strata (Tschopp, 1953) and estimates of weighted mean formation thermal conductivity (λ) for the Oriente basin, Ecuador

Locality	Formation	Thickness (m)	λ (W/(m K))
Cachiyaçu	Chonta	308	2.22
	Agua Caliente	78	
	Esperanza	75	
	Chushabatay	68	
Cangaime	Tena	41	2.16
	Upper Napo	71	
	Middle Napo	204	
	Lower Napo	122	
	Hollin	22	
Macuma	Tena	37	2.16
	Upper Napo	41	
	Middle Napo	185	
	Lower Napo	122	
	Hollin	54	
Villano	Tena	27	2.22
	Upper Napo	41	
	Middle Napo	109	
	Lower Napo and Hollin	113	
Oglan	Tena	27	2.22
	Upper Napo	27	
	Middle Napo	48	
	Lower Napo and Hollin	203	
Vuano	Tena	51	2.32
	Upper Napo	27	
	Middle Napo	61	
	Lower Napo and Hollin	248	
Coca	Tena	7	2.19
	Upper Napo	112	
	Middle Napo	75	
	Lower Napo and Hollin	256	
Sacha	Tena	10	2.19
	Upper Napo	122	
	Middle Napo	75	
	Lower Napo and Hollin	253	
Shushufindi	Tena	10	2.48
	Upper Napo	126	
	Middle Napo	75	
	Lower Napo and Hollin	250	
Cofane	Tena	41	2.28
	Upper Napo	129	
	Middle Napo	75	
	Lower Napo and Hollin	150	

the central parts of the continent. With the exception of the late deposits of Quaternary age, the rock formations of these basins are contiguous and constitute a rather homogeneous regional system of sedimentary sequences.

Thermal gradient data are available at present only for the Marañon and Oriente basins. Fuentes (1984) reported bottom-hole temperatures in oil wells at 46 sites in the Marañon basin. Ocola (1985) calculated temperature gradient values based on this data set and presented a preliminary gradient map of the Marañon basin. Henry and Pollack (1988) also reported values of temperature gradients by the BHT method for 15 localities in the Marañon basin, the primary data set being essentially the same as that used by Fuentes (1984). Comparative analysis of these data sets is difficult, as the relevant information concerning identification of the wells is currently not available. However, there appears to be reasonable agreement between the gradient values. Thus, the mean temperature gradient of 25.7 °C/km given by Fuentes (1984) is not significantly different from the value of 24.5 °C/km reported by Henry and Pollack (1988). More recently, Mathalone and Montoya (1995) have presented
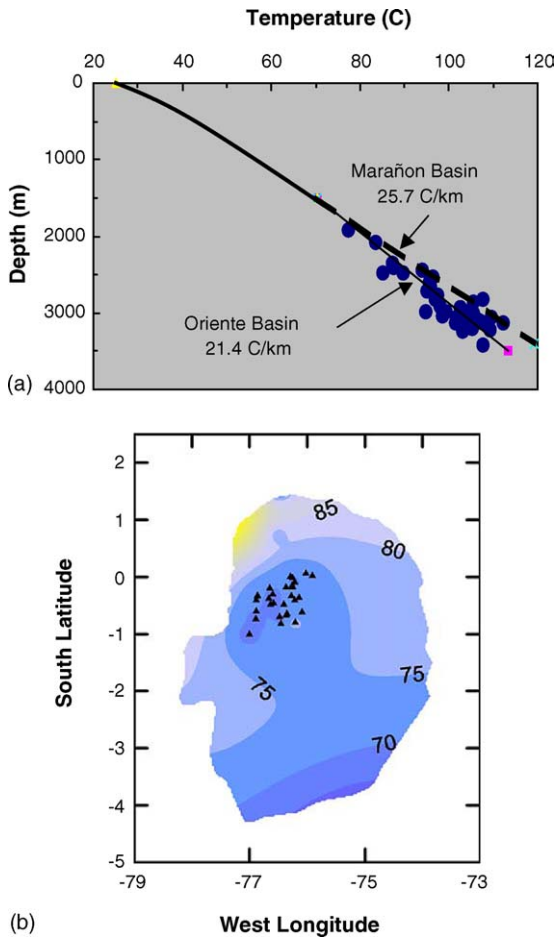
Fig. 7. (a) Bottom-hole temperatures with AAPG corrections and gradient value for the Oriente basin, Ecuador. The dashed line indicates the overall gradient value for the Marañon basin. (b) Preliminary heat flow map of the Oriente basin. The triangles are locations of heat flow measurements. The numbers on the side bar refer to heat flow values in mW/m^2.

an updated geothermal gradient map of the Marañon basin. The details of the data set employed in this latter work have not so far been published, but the regional trends in the temperature gradients are similar to those presented by Ocola (1985).

Smith (1989) refers to bottom-hole temperature data for 40 wells in the Oriente basin, which is contiguous with the northern part of the Marañon basin. Information on drilling history and circulation times of drilling fluids of these wells are currently not available. Thus, only empirical corrections, based on the depths of BHT measurements, have been attempted in the present work. The vertical distribution of bottom-hole temperatures of these wells is illustrated in Fig. 7a. Least square fits to the BHT data set with AAPG corrections indicate an overall temperature gradient of 21.4 °C/km for data from the depth

interval of 1500–3500 m. This is slightly lower than the overall gradient value of 25.7 °C/km for the Marañon basin and point to the possible existence of a systematic difference in regional geothermal pattern between these two basins.

A problem that has not been addressed properly in these earlier studies is the determination of representative thermal conductivity values of the main rock types and of the geological formations of these basins. Lack of such data has been a major obstacle in establishing basin wide correlation of thermal properties. The thermal conductivity data reported by Ocola (1985) and Henry and Pollack (1988) refers to localities within the Marañon basin. The values obtained by Ocola (1985) are found to fall in the relatively low and narrow range of 1.4–1.6 W/(m K) while those by Henry and Pollack (1988) fall in the range of 1.7–2.7 W/(m K). Both data sets refer to the same group of rock types, consisting mainly of sandstones, siltstones and shale. The thermal conductivity of such consolidated rock types fall generally in the range of 1.6–4 W/(m K), while values lower than 1.6 W/(m K) are usually encountered only for unconsolidated sediments (Clark, 1966; Kappelmeyer and Haenel, 1974). Since there are no supporting evidences for the existence of unconsolidated sediments at depths greater than 1000 m in the Marañon basin, the thermal conductivity values calculated by Ocola (1985) are considered as constituting a possible lower limit for sedimentary rocks in this area.

As for the Oriente basin, attempts were made to estimate thermal conductivity based on information available in regional stratigraphic cross-sections giving thickness and rock types of the major geological formations (Tschopp, 1953). The estimated thermal conductivity for the Cretaceous sections in the Oriente basin, based on data gathered from the lithologic profiles of deep wells, reported by Del Solar (1982) and Canfield et al. (1982) are presented in Table 7a. The conductivity values obtained are in the same range as that found in laboratory measurements by Henry and Pollack (1988) and by Springer and Foerster (1998). This overall agreement was considered satisfactory for the purposes of the present work. Heat flow values calculated using the temperature gradient data (Smith, 1989) and estimated thermal conductivity values are given in Table 7b. The preliminary heat flow map of the Oriente basin, based on the updated data set is presented in Fig. 7b.

2.8. Central parts of Colombia

The conventional heat flow database for Colombia is rather poor, there being only three measurements in

Table 7b
Bottom-hole temperatures (Smith, 1989), AAPG corrected gradients and heat flow values for the Oriente basin, Ecuador

Locality	West longitude	South latitude	Uncorrected BHT (°C)	Gradient (°C/km)	Heat flow (mW/m^2)
Auca-1	−76.8870	−0.5980	97.8	26.10	70
Auca-2	−76.8910	−0.7340	91.7	24.14	65
Capiron	−76.4800	−0.6950	91.1	25.08	68
Cononaco	−77.0000	−1.0000	95.6	24.13	65
Dicaron	−76.4570	−0.8160	95.0	25.81	70
Fanny	−76.3670	−0.1840	87.8	27.79	71
Ind. Itaya	−76.2580	−0.0200	92.2	26.23	69
Indillana	−76.5820	−0.4570	84.4	25.50	63
Joan	−76.2620	−0.1520	86.7	23.38	72
Limoncocha	−76.6640	−0.3790	94.4	26.68	69
Margaret	−76.0230	0.0630	76.7	25.71	76
Mariann-1	−76.2580	−0.1840	81.1	28.11	70
Palmeiras	−76.6020	−0.3010	87.8	24.14	65
Panacocha-B1	−76.2890	0.0040	79.4	26.48	72
Pompeya	−76.6370	−0.4770	90.6	24.48	66
Sacha-1	−76.8837	−0.4048	95.6	26.31	71
Sacha-2	−76.8721	−0.3372	96.1	26.33	71
Sacha-3	−76.8604	−0.3256	96.7	26.39	71
San Francisco-1	−76.4020	−0.4840	92.2	26.43	71
San Roque-1	−76.2190	−0.4020	87.8	26.14	71
San Roque-2	−76.2770	−0.3280	85.6	25.86	70
Shushufindi	−76.6480	−0.1950	93.9	26.64	72
Siona	−76.2150	−0.0900	76.7	24.31	66
Tangay	−76.1450	−0.3630	87.8	28.19	76
Tivacuno-3	−76.3520	−0.6480	95.6	28.25	76
Tivacuno-4	−76.3670	−0.6720	87.2	25.47	69
Vinita	−75.9140	0.0230	71.1	27.21	73
Yuturi	−76.0900	−0.6170	79.4	25.99	70
Zaparo	−76.2110	−0.7970	97.8	29.22	79

the northwestern parts, close to the border with Panama (Sass et al., 1974). This is an area located to the west of the cordilleran region, where recent magmatic activities associated with subduction processes are less pronounced. Obviously, these values cannot be considered as representative of the thermal regime of the Cordilleran regions in the central and eastern parts of Colombia, characterized by the presence of large belts of active volcanism. During the last decade, new geothermal data has been acquired in south central parts of Colombia (OLADE, 1982, 1987). Alfaro and Bernal (2000) in reporting results of a geothermal reconnaissance study of the Azufral area presented geochemical thermometric data for nine localities. They also estimated temperatures of deep seated aquifers, making use of four different aqueous geo-thermometers. This data has been used

Table 8a
Estimates of heat flow for the Azufral area, southwestern Colombia, based on the geochemical method

Locality	Coordinates		Temperature (°C)		Heat flow (mW/m^2)
	Longitude	Latitude	Outflow	Silica	
San Ramon	−77.6800	1.0800	31	153	189
La Cabaña	−77.6820	1.0830	24	129	154
El Salado de Malaber	−77.6830	1.0820	25	144	176
Malaber 1 Sapuyes	−77.6790	1.0810	32	156	194
Malaber 2 Sapuyes	−77.6810	1.0790	32	155	192
Quebrada Blanca (2)	−77.6800	1.0800	50	169	213
El Baño (3)	−77.6840	1.0810	48	177	225
Laguna Verde	−77.6830	1.0870	–	148	182

The numbers in brackets refer to groups of springs (Alfaro and Bernal, 2000; Alfaro, personal communication).

Table 8b
Estimates of BHT gradients (Alfaro et al., 2000) and plausible range of heat flow values for the pericratonic basins in western Colombia

Region	No. wells	Mean gradient (°C/km)	Heat flow (mW/m^2)
Nevado de Ruiz	49	32	64–76
Caguan Vaupes	12	40	80–120
Catatumbo	53	30	60–90
Cauca Patia	2	23	46–69
Cesar Rancheria	7	32	64–96
Eastern Range	15	28	56–84
Guajira	40	19	38–57
Llanos Orientales	322	26	52–72
Putumayo	166	28	56–84
Tumaco	2	21	42–63
Uraba	6	17	34–51
Lower Magdalena	131	24	48–72
Middle Magdalena	615	20	40–60
Upper Magdalena	292	27	54–81

recently (Alfaro, personal communication) in obtaining estimates of heat flow based on the geochemical method. These estimates are presented in Table 8a.

More recently, Alfaro et al. (2000) reported temperature gradient values for thirteen sedimentary basins in central parts of Colombia. These are based on BHT measurements carried out in 1712 deep wells drilled as part of oil exploration in the pericratonic basins. Details of the primary data set with information on depth and drilling history are not available at present and hence corrections for gradient values have not been attempted. Most of the wells have depths less than 3000 m and consequently standard corrections, such as AAPG, are expected to have magnitudes not exceeding 10% of the reported mean values.

Thermal conductivity measurements have not so far been carried out for samples from these wells. Macellari (1988) carried out a comprehensive analysis of the sedimentary sequences occurring in a number of pericratonic basins in central Colombia. The main rock types in these basins are shales, sandstones and carbonates. Examination of published information on cross-sections of sedimentary sequences of these basins points to a predominance of clastic sediments with comparable proportions of sandstone and shale. Such mixtures are generally characterized by thermal conductivity values in the range of 1.5–4.5 W/(m K), with mean values falling in the more restricted interval of 2–3 W/(m K). Such estimates were used in setting plausible upper and lower limits of heat flow values, given in Table 8b. We consider the lower limits as more reliable indicators of regional heat flow. With the exception of Caguan

Vaupes region the lower limits are in the range of 30–60 mW/m^2, in reasonable agreement with the heat flow values found for the Pre-cordilleran basins to the south. In view of the uncertainties in such estimates no attempt has been made to map distribution of heat flow in central Colombia. However, it is important to point out that the adjacent regions to the west of these basins are affected by recent magmatic activity. Results of geological and geochemical studies point to the existence of a belt of anomalous thermal regime along the southwest-northeast direction, coincident with the zone of active volcanism and widespread hydrothermal manifestations at the surface. This magmatic belt also extends southward into the cordilleran region of Ecuador.

3. Regional distribution

The non-uniform distribution of heat flow data in relation to the large scale-geological structures continue to be a major obstacle in understanding regional variations in the geothermal regime of South American continent. The variability in quality of the available data set is also a factor that has some influence on our understanding of the regional distribution. It is, in part, related to the characteristics of the different methods used for determining heat flow, which in turn depend on the nature and availability of primary geothermal data. Care need to be taken in employing such data sets of mixed quality in evaluating regional heat flow. Following Hamza and Muñoz (1996) a priority scheme has been adopted, based on qualitative considerations of the relative advantages and disadvantages of the various methods.

Not withstanding the quality considerations, the current data set has allowed estimates of heat flow for 42 out of 52 regional structures. Mean heat flow values for the main tectonic units are presented in Table 9. In view of the inherent uncertainties in the estimated values by geochemical methods, two sets of mean values were calculated: one based on the entire data set and a second one based on a reduced data set in which the estimated values by geochemical methods have been eliminated. The mean values based on the reduced data set may be considered as representative of regional heat flow in tectonically quiescent areas, which include Pre-cordilleran basins in the west and the Brazilian Platform in the east. On the other hand, the mean values based on the mixed data set are likely to be representative of regional heat flow in areas of recent tectonic and magmatic activity, mainly the Andean cordilleran regions in the west.

The geographic distribution is relatively better for structures belonging to the southern parts of the Brazilian Platform and the central parts of Andean Region. It

Table 9
Mean heat flow values for some of the principal regional structures in South America

Structural unit	Mean heat flow (mW/m^2)			
	N_o	q_o	N_R	q_R
Cordilleran regions	252	103 ± 78	128	59 ± 32
Pre-cordilleran ranges and basins	129	54 ± 25	110	44 ± 11
Cratonic areas and fold belts	152	65 ± 23	84	59 ± 23
Phanerozoic interior basins	231	63 ± 23	207	58 ± 20
Mesozoic coastal basins	22	58 ± 10	20	59 ± 10
Post mesozoic rift basins	46	84 ± 26	39	82 ± 27
Northern basins and depressions	2	106 ± 24		
Patagonian platform	6	74 ± 13	3	76 ± 21
Total	840	74 ± 51	591	59 ± 30

'N' is the number of data and q is the heat flow. The subscripts "o" refers to the entire data set while "R" refers to the reduced data set in which estimated values based on geochemical methods have been excluded.

is modest to poor elsewhere. Heat flow is found to be variable in the cordilleran region, with the eastern and southern parts having relatively high values compared to the western and northern parts. There is a general trend of increasing heat flow, from the western coastal area towards the cordilleras. Thus, it is common to find heat flow as low as 25 mW/m^2 in the coastal zones, while values of over 100 mW/m^2 are encountered in the Altiplano. In the Pre-cordilleran basins, to the east of the main cordilleras, heat flow is low to normal. The overall picture thus seems to be typical of the thermal pattern predicted by the plate tectonic theory for ocean – continent convergence zones.

In the eastern part of the continent heat flow is low to normal (<75 mW/m^2) in most parts of the Brazilian Platform. Lowest values (less than 50 mW/m^2) are encountered in cratonic regions while the Proterozoic fold belts are found to have heat flow in the range 45–75 mW/m^2. Nevertheless, some higher values have been found to occur in limited portions of over-thrust regions in the Precambrian fold belts. Heat flow is low to normal (in the range of 50–70 mW/m^2) in most of the intracratonic basins in the Brazilian Platform and in the eastern parts of the Patagonian Platform. Notable exceptions are the Mesozoic rift basins (Potiguar, Recôncavo and Taubaté) where heat flow is relatively high (>80 mW/m^2).There are some indications that heat flow relatively high in the western parts of the Patagonian Platform relative to its eastern parts.

A closer examination of the data set reveals that the thermal field is not uniform within individual tectonic units. In fact, variability in heat flow is found to occur even within segments with relatively uniform seismic, gravity and magnetic signatures. There are indications that a large part of intra-structural variations arise from complexities associated with local geologic structures,

such as thermal refraction effects or changes arising from the non-homogeneous distribution of radiogenic heat production (Vitorello et al., 1980; Hamza, 1982a). In some areas, deep circulation of meteoric waters through either permeable strata or fracture zones has lead to distortions in the temperature field and heat flow pattern. On the other hand, a large part of inter-structural variability seems to originate from deep-seated tectonic processes.

4. Polynomial representation of regional heat flow field

Polynomial (or trend surface) analysis is usually recommended for examining heat flow patterns of areas, generally not exceeding the size of continents (Cermak, 1983). In this method, the spatial distribution of heat flow is represented by a polynomial of selected order of expansion, the coefficients of which are determined using a system of equations, corresponding to the number of measured values. This in turn allows calculation of the trends of surface heat flow depending on the order of expansion of the polynomial (Haenel, 1971; Vasseur and Nouri, 1980). The approach is based on the assumption that a polynomial surface is an adequate representation of the regional trend (Agocs, 1951; Simpson, 1954). The regional trends are, in general, represented by low order polynomial surfaces. However, Beltrão et al. (1991) argue that adequate representation of simple anomalies may also require higher order polynomials.

Least square methods are usually employed in the fit of the trend surface. In the present work, the procedure adopted is analogous to that used by Abdelrahman et al. (1985) where the choice of the optimum degree is based on analysis of variance. There are however, some difficulties, such as the appearance of pseudo-anomalies and sensitiveness to the presence of 'outliers'. The

appearance of pseudo anomalies, which is intrinsic to most of the least square methods, is controlled by choosing discrete intervals for representation of polynomial surfaces. The problem arising from sensitiveness to 'outliers' is minimized by taking into consideration complementary information on geological characteristics of the area under consideration and careful pre-screening of the observational data set. In the present case, the computer implementation of the trend surface analysis by least squares method was carried out using a modified version of the algorithm by Malin et al. (1982). Trend surface maps were generated subsequently using commercially available software packages such as GMT (Wessel and Smith, 1992) and SURFER (Golden Software Inc., 2002).

An important point to be considered in this context is the influence of data quality in polynomial representations. Thus, an approach similar to that of Hamza and Muñoz (1996) has been adopted in the present work as well, where priority is attributed to data acquired using conventional (CVL) and bottom-hole temperature (BHT) methods. Estimates of heat flow based on the geochemical (GCL) methods are considered to be of low quality and are taken into consideration only for regions of low data density. Between these extremes are the heat flow determinations carried out using the underground mine (MGT) and aquifer temperature method (AQT) and those acquired using oceanic heat flow techniques (OHF) in shallow inland water bodies. As pointed out by Hamza and Muñoz (1996) the benefits of retaining low quality heat flow values in areas of poor data density often outweigh the more serious problems arising from the uneven geographic distribution of the data set. In particular, the low quality data sets provide useful constraints for outlining regional trends in areas of poor data density. This is essentially similar to the approach employed in elaboration of global heat flow maps (Chapman and Pollack, 1975; Pollack et al., 1993).

In order to examine the effects of variability in data quality two different data sets were employed in polynomial analysis. The first is a reduced data set, where only heat flow values obtained by conventional and BHT methods are considered. The second is a mixed data set that includes, in addition, a selected set of estimated values. The estimated values are admitted only for areas of poor data density. As an example of the results obtained we present in Fig. 8a and b the first order polynomial representations of the heat flow pattern based on the reduced and mixed data sets respectively. Note that the first order representation exhibit similar features in both cases. The range of heat flow values is however higher for the representation based on the mixed data set. This

is a consequence of the fact that the mixed data set includes estimates for geothermal areas, which are in general characterized by higher heat flow values.

It appears that the differences in polynomial representations of the two data sets become significant as the order of the expansion increases. Consider, for example, the fourth order representations of the reduced and mixed data sets, presented in Fig. 8c and d. The fourth order representation based on the reduced data set (Fig. 8c) indicates a simple pattern characterized by low heat flow ($<50 \, mW/m^2$) in a broad region in the northern parts and normal heat flow (50–$80 \, mW/m^2$) for the remaining parts of the continent. On the other hand, the fourth order representation based on the mixed data set (Fig. 8d) point to a distinctly different pattern of heat flow, where the size of low heat flow region in the northern parts of the continent is smaller. In addition, it points to the existence of several high heat flow areas in the southern parts and also in the northern coastal area. However, the most outstanding difference stems from the fact that the fourth order representation in Fig. 8c is practically incapable of identifying the regions of high heat flow in the cordilleran regions. The one based on the mixed data set (Fig. 8d) is more successful in identifying the main geothermal areas along the western parts of the continent.

The first order representations (Fig. 8a and b) are just plane surfaces indicative of a systematic increase in heat flow in the north-south direction. This is an important feature, which seems to point to the existence of a deep-seated heat transfer process. Among a number of possible mechanisms, we consider here the one related to the systematic differences in heat flow between oceanic and continental regions, as the most likely. Jessop et al. (1976) pointed out that mean heat flow in oceanic segments of the lithospheric plates is in general higher than that of their continental counterparts. Consequently, one may expect an inverse relation between regional heat flow and the area of continental segment. The implications of the relations between area, age and heat flow in oceanic regions have been discussed in the literature (see, for example, Parsons, 1982; Stein and Stein, 1992). More recently, Grigné and Labrosse (2001) have considered the thermal blanketing effect of continents on mantle heat flow. Thus, the systematic trend of increasing heat flow, revealed in polynomial representations, may be considered as related to the overall decrease in surface area of the South American continent, in the north-south direction.

The fourth degree polynomial representations (Fig. 8c and d) provide better insights into the regional heat flow pattern. Prominent among these are east-west trending belts of low heat flow in northern Peru and in central
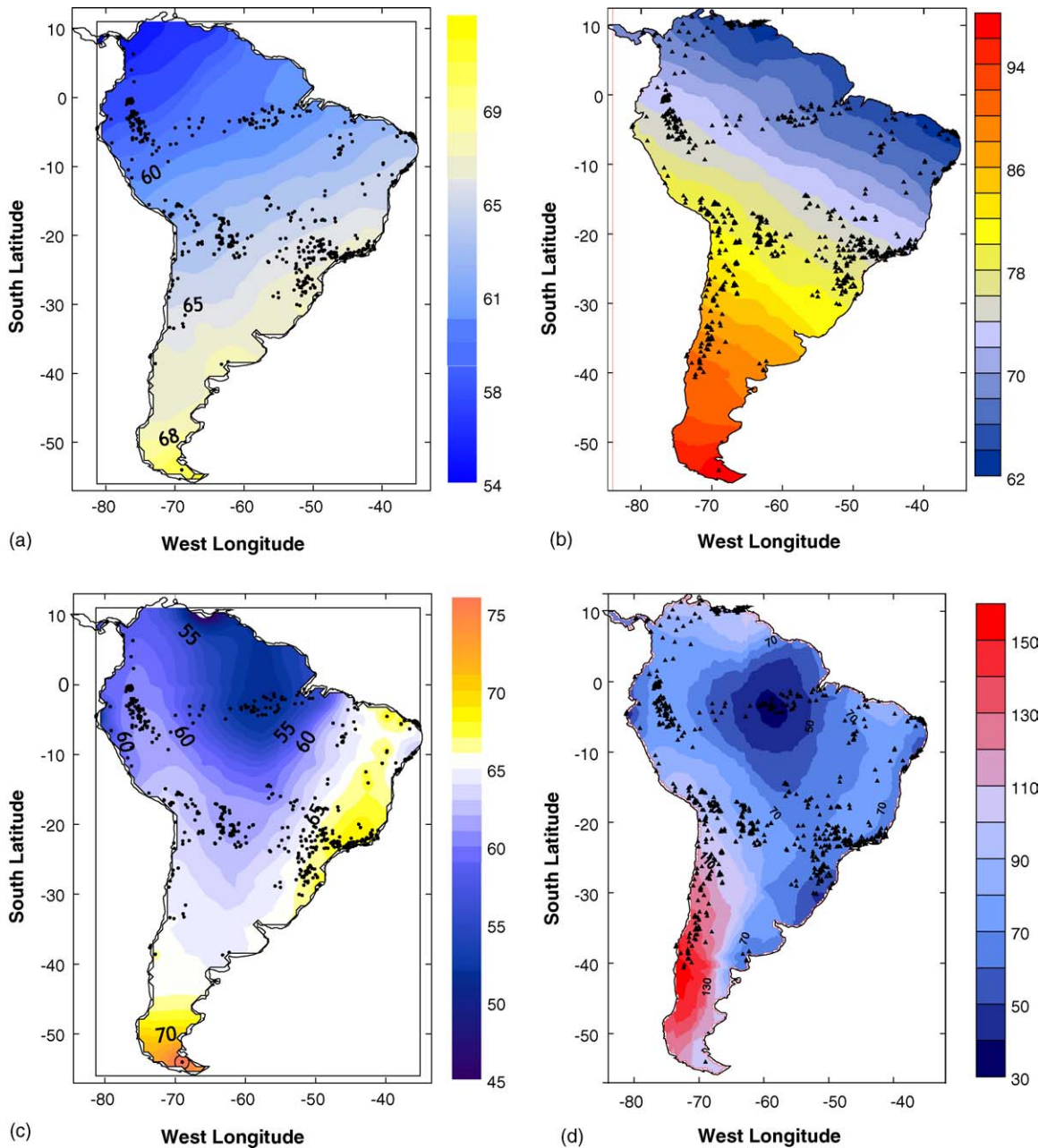
Fig. 8. (a) First order polynomial representation of heat flow in South America, based on conventional and BHT data sets. The points are locations of heat flow measurements. (b) First order polynomial representation of heat flow in South America, based on data set of mixed quality (see text for details). The points are locations of heat flow measurements. (c) Fourth order polynomial representation of heat flow in South America, based on conventional and BHT data sets. The contour interval is 5 mW/m^2. (d) Fourth order polynomial representation of heat flow in South America, based on data set of mixed quality (see text for details). The contour interval is 10 mW/m^2. The points are locations of heat flow measurements.

Chile, as well as the high heat flow belts in northern Chile, Altiplano of Bolivia and northwestern Argentina. The presence of high heat flow along cordilleras in the southern parts (including the western margin of the Patagonian Platform) and areas comprising Venezuelan Andes in the northern parts of the continent are clearly

seen in fourth order representations. The failure to identify major geothermal areas in central Colombia and Ecuador appear to originate from poor data density.

Comparison with the manual and automatic contour maps presented by Hamza and Muñoz (1996) indicates that the polynomial representation has filtered out short
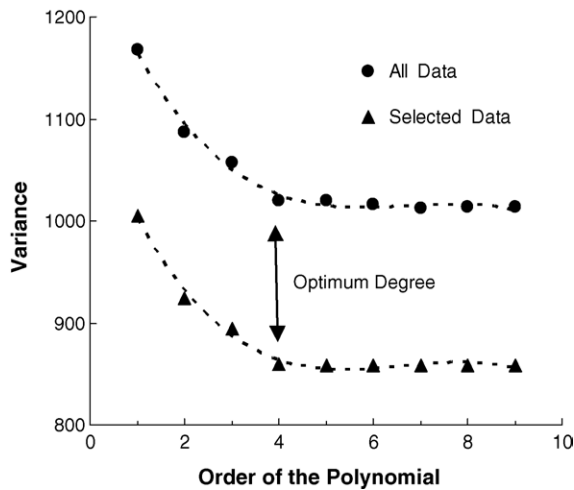
Fig. 9. Change of variance with the degree of polynomial. The arrow indicates the degree of the polynomial at which the change in variance becomes insignificant.
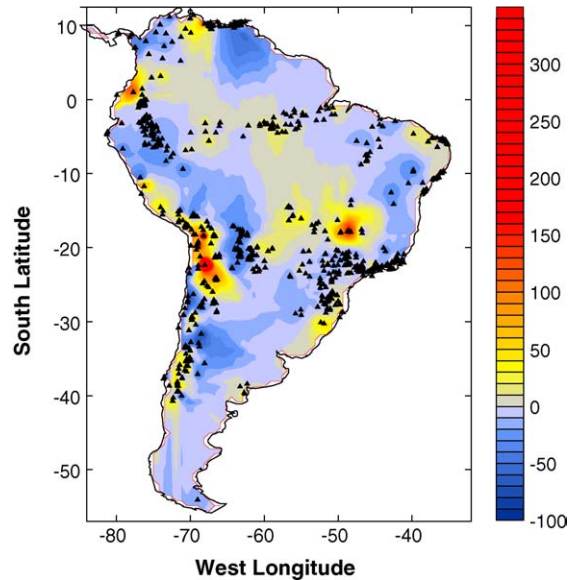

Fig. 10. Residual anomalies of fourth order polynomial representation relative to observed values of heat flow in South America. The triangles indicate locations of heat flow measurements. The contour interval (see side bar) is $10\,mW/m^2$.

wavelength anomalies. Large variations in data density have also lead to elimination of some of the structurally important features outlined in the manual contour maps of observational data. However, manual contour maps usually take into consideration supplementary geologic information. Recognition of some of these small-scale features is possible by increasing the order of the polynomial. However, limitations arising from low data density and uneven geographic distribution warrant higher order representations.

In this context, it is convenient to comment on the choice of optimal degree of the polynomial representation. Abdelrahman et al. (1985) and Zeng (1989) suggested procedures, which use the mean square deviation between the calculated and observed values as a suitable criterion. In the present case, the variation of the mean square deviation with the order of the polynomial is illustrated in Fig. 9. In this figure, the solid circles refer to the case in which the mixed data set is employed in the trend surface analysis. It is obvious that fourth order representation is a reasonable choice, as the change in variance is relatively small for higher order representations. However, the mean variance for this case is relatively large, in the range of 1000–1200. Improvements in the variance can be achieved by imposing quality criteria in the selection of data. Thus, the triangles in Fig. 9 refer to results of trend surface analysis of the reduced data set where estimates based on the geochemical methods are excluded. In this case, the mean variance falls to the range of 800–1000 while the optimum degree of the polynomial has remained at about the same value of four. Again, higher order representations are unwarranted.

A complementary form of extracting additional information on small-scale variations is to examine the differences between the regional field and the observed values. Consider for example the residual components relative to the fourth order representation of the mixed data set. The geographic distribution of these residuals is presented in the map of Fig. 10. In this map, it is easier to identify such features as the low heat flow zones in northern Peru and central Chile and the high heat flow zones in the southern Andes and in the Altiplano. The map of residual anomalies is also successful in identifying areas of higher than normal heat flow in the south-central and northeastern parts of Brazil. Most of the Brazilian platform, comprising cratonic areas and Precambrian fold belts, has low to normal heat flow. Thus, in spite of problems associated with quality and non-uniform distribution the polynomial representations can be considered as providing a reasonably reliable picture of the regional heat flow pattern in the South American continent.

5. Discussion and conclusions

Improvements brought in by the new data sets provide better insights into the nature and characteristics of heat flow variations in central and southern parts of the Brazilian Platform, central Andean region, Chaco Plains, Paraná basin in the south and Pre-cordilleran basins in the north. Examination of regional variations indicate that the heat flow fields of wide tectonically

active plateaus associated with high-angle subduction zones are distinctly different from those of the narrow non-volcanic cordilleras overlying the low-angle subduction zones. For example, the elongated east-west trending belts of low heat flow in northern Peru (between latitudes 5 and 15°S′) occur in a region where active volcanism is absent and where, according to several studies (e.g., Cahill and Isacks, 1992), a flattening of the Wadati-Benioff zone is observed. It is possible that low heat flow values in the cordilleran regions in Peru are a consequence of under-thrusting of cold oceanic crust eastward of the trench line in western South America. Thermo-mechanical models proposed in the literature (see, for example, Van den Beukel and Wortel, 1987, 1988) indicate that low heat flow can persist for distances of only up to several hundred kilometers from the trench line. The high heat flow areas of Altiplano and Puna blocks are characterized by high values of (anelastic) attenuation while relatively low values of attenuation are observed in areas of low heat flow. Results of geo-electromagnetic soundings in the high heat flow areas of central Andes by Muñoz et al. (1992) and Schwarz et al. (1994) indicate the presence of extremely high values of electrical conductance. Such observations may be considered as indications of anomalous thermal conditions prevailing in the subcrustal lithosphere.

On a broader scale, the trend surface maps of heat flow presented here may be considered as providing an overall view of large-scale heat flow variations within the South American continent. For example, the north-south trend of increasing heat flow is a feature that was not identified clearly in earlier mapping efforts. The features discernible in higher order representations appear to be related to the characteristic features of the subduction processes going on the western margin of the continent. The maps of residual anomalies relative to low order trend surfaces have allowed identification of several new features in the regional geothermal regime. Analysis of residual anomalies can serve as a convenient starting point for detailed geothermal investigations on local scales. The results also indicate that further improvements in polynomial and numerical representations of regional thermal fields can only be achieved through acquisition of new geothermal data in areas of low data density.

Acknowledgments

Appendix A. Description of procedures used in determination of geothermal heat flux

A.1. Experimental techniques

Bead type thermistors (YSI Inc.) were used as sensors for temperature measurements in boreholes. The probes containing sensors are connected to a 6.5 digit (Hewlett-Packard) resistance-measuring device via three conductor coaxial copper cables with appropriate electrical insulation. The logging equipment, similar in construction to the one described by Beck (1963), are manually operated. The overall response of the equipment was calibrated using platinum resistance thermometer (Presys ST-501 with ITS-90 specifications). In most temperature logs, measurements were made at two-meter intervals during the down-going operations.

The methods used for the determination of thermal conductivity of rock samples from Brazil may be classified as falling into two groups, namely line source and plane source. The principles of line source method and details of experimental arrangements are discussed in the literature (see, for example, Beck, 1988). Some of the probes were locally built and compared against standard probes (such as the ones by Fenwall Electronics). In the present case, depending on the nature of rock samples available, two different heat flux geometry were employed, designated here as *full-space* and *half-space*. Full-space configuration was employed in the case of unconsolidated samples and drill cuttings, where the needle probe is inserted into the sample. Half-space configuration was employed for the case of solid samples and drill cores, where the needle probe glued onto the surface of a low-conductivity reference plate is brought into contact with the polished surface of the sample during measurements. A set of primary (fused silica and crystalline quartz) and secondary (materials for engineering studies) standards of known thermal conductivity were employed in the calibration of the experimental devices. Measurements were carried out on samples under dry and vacuum saturated conditions.

Carslaw and Jaeger (1959) discuss the principle of the plane source method in detail. The temperature (T) vari-

ation with time (t) of a sample of thermal conductivity (λ) in contact with a continuous plane source of heat is given by:

$$T = Q\left(\frac{t\rho C}{\pi\lambda}\right)^{1/2} \mathrm{e}^{-(x-x')^2/4\kappa t}$$
$$- \frac{Q|x-x'|}{2\kappa\rho c}\mathrm{erfc}\frac{|x-x'|}{2\sqrt{\kappa t}} \tag{A.1}$$

where Q is the strength of heat source, ρC the heat capacity and κ is the thermal diffusivity. Mongelli (1968) reported results of experimental studies on rock samples using this method. In the present work, a commercially available version of the instrument (ISOMET, Applied Precision, Slovakia) was used. This instrument is equipped with a microprocessor device, which carries out the integration of the time–temperature curves and provides a display of the calculated value of thermal conductivity. Integration of the thermal response is carried out during both heating and cooling cycles.

A.2. Methods employed in determining heat flow

A.2.1. Conventional (CVL) method

This is the traditional method of determining terrestrial heat flow in boreholes with large sections of homogeneous rock type and undisturbed thermal regime. The gradient values were calculated by least square fits to temperature data from selected depth intervals. For N pairs of depth (z) – temperature (T) data the least square estimates of gradient (Γ) and intercept (T_0) are given by the relations:

$$\Gamma = \frac{N\sum z_i T_i - \sum z_i \sum T_i}{N\sum z_i^2 - (\sum z_i)^2} \tag{A.2}$$

$$T_0 = \frac{\sum z_i^2 \sum T_i - \sum z_i \sum z_i T_i}{N\sum z_i^2 - (\sum z_i)^2} \tag{A.3}$$

The thermal conductivity (λ) was calculated by arithmetic or harmonic averaging, the latter one gives rational results:

$$\lambda = \frac{\sum d_i}{\sum d_i/\lambda_i} \tag{A.4}$$

where d_i is the thickness of the layer i. The heat flow is calculated as the simple product of least square temperature gradient (A.1) and harmonic mean thermal conductivity (A.3). The standard deviation of heat flow (σ_q) is calculated from the standard deviations of gradient (σ_Γ) and the thermal conductivity (σ_λ):

$$\sigma_q = \sqrt{\Gamma^2\sigma_\lambda^2 + \lambda^2\sigma_\Gamma^2} \tag{A.5}$$

The method is well-known since the pioneering works of Everett (1868–1895), warranting further details. In the present work, conventional method (CVL) was employed in determination of heat flow in the coastal area of southeastern Brazil.

A.2.2. Bottom-hole (BHT) and conventional bottom temperature (CBT) methods

Both of these methods are actually simple variations of the thermal resistance method, originally proposed by Bullard (1939). The bottom-hole temperature method (BHT), initially proposed by Carvalho and Vacquier (1977), has been widely used for determining heat flow in sedimentary basins. The method may also be adapted for determination of heat flow in boreholes perturbed by in-hole fluid flows. In the present work, this approach is designated as the *conventional bottom temperature method* (CBT). It is practically identical to the BHT method used in oil wells. The main difference is that the bottom temperatures in CBT method may be measured with better accuracy and, in addition, repeat measurements carried out with ease.

In both cases (BHT and CBT) the temperatures at the bottom of the well (T_{BHT}) and the mean annual surface temperature (T_0) are used in determining an apparent temperature gradient (Γ) using the relation:

$$\Gamma_{\mathrm{BHT}} = \frac{T_{\mathrm{BHT}} - T_0}{Z_{\mathrm{BHT}} - Z_0} \tag{A.6}$$

The heat flow is calculated, under the assumption of steady state conditions:

$$q = \frac{T_{\mathrm{BH}} - T_0}{\sum_{i=1}^{N}(Z_i/\lambda_i)} \tag{A.7}$$

where Z_i is the thickness of the layer with thermal conductivity λ_i and N are the number of layers. The summation in the denominator represent the cumulative thermal resistance of rock types in the bore hole up to the depth at which T_{BH} is measured.

In the present work, BHT method was employed for determining heat flow in oil wells drilled in the Paraná, Chaco, and Oriente basins. CBT method was employed for determining heat flow in shallow boreholes in the southeastern coastal area of Brazil.

A.2.2.1. Corrections to BHT data. The bottom-hole temperature data need to be corrected for the effects of drilling disturbances. Ribeiro and Hamza (1986) discussed advances in theory and practice of BHT corrections and pointed out possible improvements for the models currently in use. The corrections calculated by Eston et al. (1983), based on the line source (see, for

example, Lachenbruch and Brewer, 1959) and the circular well (Middleton, 1979; Leblanc et al., 1980) models of drilling disturbances. In these models, the respective corrections are calculated using the relations:

$$T_{BHT} = T_F + \Delta T \left[\ln \left(1 + \frac{t_C}{t_S} \right) \right] \tag{A.8}$$

$$\frac{T_{BHT} - T_m}{T_f - T_m} = 1 - \exp \left[\frac{-a^2}{4 \kappa t} \right] \tag{A.9}$$

where T_{BHT} is the measured value of temperature at the bottom of the well, T_F the undisturbed formation temperature, ΔT the magnitude of the perturbation, t_C the time of mud circulation in the well, t_S the time elapsed after mud circulation, a the radius of the well and κ is the thermal diffusivity. A basic requisite for applying such corrections is the availability of multiple time-temperature data, after cessation of drilling activities.

In the absence of such multiple time–temperature data sets, empirical correction procedures are attempted. In the present work, the relation proposed by AAPG (1976) was adopted in calculating corrections to BHT data:

$$\Delta T = az + bz^2 - cz^3 - dz^4 \tag{A.10}$$

where ΔT is the temperature correction, z the depth and a–d are the coefficients of the polynomial with values 1.878×10^{-3}, 8.476×10^{-7}, 5.091×10^{-11} and 1.681×10^{-14}, respectively.

A.3. Aquifer temperature (AQT) method

This method, originally proposed by Santos et al. (1986), is useful for determining thermal gradients in wells where the presence of pumping equipment does not allow log operations. The procedure is based on the relation (Bolditzar, 1958) between aquifer temperature (T_A) and temperature of pumped water (T_W):

$$\frac{T_W - T_0}{T_A - T_0} = M'R \left[1 - \exp \left(\frac{-1}{M'R} \right) \right] \tag{A.11}$$

where T_0 is the mean annual surface temperature, $M' = MC/\lambda H$ the dimensionless mass flow rate (M being the mass flow rate during pumping tests, C the specific heat of water, λ the thermal conductivity of rock formations at the site of the well and H the depth of the aquifer) and R a parameter given by Birch (1947):

$$R = \left(\frac{1}{4\pi} \right) \int_{r^2/4\kappa t}^{\infty} Z^{-1} \exp(-Z) I_0(Z) \, dZ \tag{A.12}$$

In Eq. (A.12), r is the radius of the well, κ the thermal diffusivity of the rock formation, t the time since pumping started and I_0 is the modified Bessel function of the

first kind of order zero. In Eq. (A.11), the left hand side represents the dimensionless temperature (θ). It is fairly simple to note that T_W approaches T_A when the pump rate is large and the aquifer not very deep. Also, as has been pointed out by Santos et al. (1986), the variations in thermal conductivity of the wall rocks have only very small effect on the temperatures of the pumped water.

References

Agocs, W.B., 1951. Least-squares residual anomaly determination. Geophysics 16, 686–696.

Abdelrahman, E.M., Rias, S., Refai, E., Amin, Y., 1985. On the least-squares residual anomaly determination. Geophysics 50, 473–480.

Alfaro, C., Bernal, N., 2000. Geothermal reconnaissance study at Azufral Volcano (extended abstract). In: 31st Geological Congress, Rio de Janeiro, Brazil, pp. 34–39.

Alfaro, C., Bernal, N., Ramirez, G., Escovar, R., 2000. Colombia, country update. In: Proceedings World Geothermal Congress, Kyushu-Tohoku, Japan, pp. 45–54.

American Association of Petroleum Geologists (AAPG), 1976. Basic data file from AAPG Geothermal Survey of North America. University of Oklahoma, Norman.

Anjos, C.E., Veneziani, P., 1977. Application of remote sensing in the study of geothermal anomaly in the municipality of Caldas Novas – Goiás (in Portuguese). Publication 1129. National Institute of Space Research, INPE, São José dos Campos, Brazil, pp. 1–114.

Beck, A.E., 1963. Lightweight borehole temperature measuring equipment for resistance thermometers. J. Sci. Instr. 40, 452–454.

Beck, A.E., 1988. Methods for determining thermal conductivity and thermal diffusivity. In: Haenel, R., Rybach, L., Stegena, L. (Eds.), Handbook of Terrestrial Heat Flow Density Determination. Kluwer Academic Publishers, Dordrecht, pp. 87–124.

Beltrão, J.F., Silva, J.B.C., Costa, J.C., 1991. Robust polynomial fitting method for regional gravity estimation. Geophysics 56, 80–89.

Birch, F., 1947. Temperature and heat flow in a well near Colorado Springs. Am. J. Sci. 245, 733–753.

Birch, F., 1948. The effect of Pleistocene climate variations upon geothermal gradients. Am. J. Sci. 246, 729–760.

Bolditzar, T., 1958. The distribution of temperatures in flowing wells. Am. J. Sci. 256, 294–298.

Bullard, E.C., 1939. Heat flow in South Africa. Proc. Roy. Soc. Lond. Ser. A. 173, 474–502.

Bullard, E.C., 1940. The disturbance of the temperature gradient in the earth˘s crust by inequalities of height. Month. Not. Roy. Astr. Soc. Geophys. Suppl. 4, 300–362.

Cahill, T., Isacks, B.L., 1992. Seismicity and shape of the subducted Nazca plate. J. Geophys. Res. 97, 17503–17529.

Calvi, E., Grassi, S., Hamza, V.M., 2000. Geochemical reconnaissance of some hydrothermal prospects in the states of Goiás and Tocantins, central Brazil, unpublished report. IIRG, Pisa, Italy, pp. 1–22.

Campos, E.C., Costa, J.F.G., 1980. Hydrogeology project of the region of Caldas Noas (in Portuguese), Final Report, vol. 1. Companhia Pesquisa de Recursos Minerais – CPRM, Goiânia, Brazil, pp. 1–123.

Canfield, R.W., Bonilha, G., Robbins, R.K., 1982. Sacha oil field of the Ecuadorian Oriente. Bull. Am. Assoc. Petrol. Geol. 66, 1076–1090.

Carslaw, H.S., Jaeger, J.C., 1959. Conduction of Heat in Solids, second ed. Oxford University Press, London, 510p.

Carvalho, H.S., Vacquier, V., 1977. Method for determining terrestrial heat flow in oil fields. Geophysics 42, 584–593.

Cavalcante, A.S.B., 2003. Paleoclimate variations in Brazil on the basis of geothermal method (in Portuguese), Unpublished M.Sc. Thesis. National Observatory, Rio de Janeiro, Brazil, p. 129.

Cermak, V., 1983. The construction of heat flow density maps. Zbl. Geol. Palaont. Teil I H1/2, 57–69.

Cermak, V., Hurtig, E., 1979. Heat flow map of Europe. In: Cermak, V., Rybach, L. (Eds.), Terrestrial Heat Flow in Europe, Color Enclosure. Springer Verlag, Berlin, Heidelberg, New York.

Cerrone, B.N., Hamza, V.M., 2003. Climate changes of the recent past in the state of Rio de Janeiro, based on geothermal method (in Portuguese). In: International Congress of the Brazilian Geophysical Society, SBGf, Rio de Janeiro, Brazil.

Chapman, D., Pollack, H., 1975. Global heat flow: a new look. Earth Planet. Sci. Lett. 28, 23–32.

Clark Jr., S.P. (Ed.), 1966. Handbook of Physical Constants, vol. 97. GSA Memoir, p. 587.

Comin-Chiaramonti, P., De Min, A., Marzoli, A., 1996. Magmatic rock-types from the Asunción – Sapucai Graben: chemical analyses (Appendix II). In: Comin-Chiaramonti, P., Gomes, C.B. (Eds.), Alkaline Magmatism in Central – Eastern Paraguay: Relatonships with Coeval Magmatism in Brazil. Universidade de São Paulo, São Paulo, Brazil, pp. 331–347.

Dardenne, M.A., 2000. The Brasilia fold belt. In: Cordani, U.G., Milani, A.J., Thomaz Filho, A., Campos, D.A.R. (Eds.), Tectonic Evolution of South, America, 31st International Geological Congress, Rio de Janeiro, Brazil, pp. 231–264.

Del Solar, C., 1982. Ocurrencia de hidrocarburos en la formación Vivián, nororiente Peruano. In: I Simposio Exploración Petrolera en las Cuencas Subandinas, vol.1. Asociación Colombiana de Geólogos y Geofísicos del Petroleo, Bogotá.

Dos Anjos, I.L.S., Vasconcellos, R.M. de, 2000. Magnetic Map of the State of Rio de Janeiro – Analytic Signal of the Magnetic Field, Scale 1:5.00.000 (in Portuguese), Projeto Rio de Janeiro. CPRM, Serviço Geológico do Brasil, Rio de Janeiro.

Duarte, H.S.B., Soares, W.G., Alencar, M.L.A, Gurvitz, H., Pires, Z.S., Santo, C.R.R. e Shimizu, M., 1978. Climatological Indicators of the State of Rio de Janeiro (in Portuguese). Publication FIDERJ, Diretoria de Geografia e Estatística, p. 156.

Eston, S.M., Hamza, V.M., Becker, E.A., 1983. Geothermal research for oil exploration in the Paraná basin (in Portuguese), Report No. 18271. Institute for Technology Research of the State Government of Sao Paulo–IPT, pp. 138.

Everett, J.D., 1868–1895. Report of the committee for the purpose of investigating the rate of increase of underground temperature downwards in various localities of dry land and under water. Rep. Br. Ass. Advmt. Sci. (most years).

Ferreira, L.E.T., 2003. Assessment of Geothermal Resources of the State of Goiás, Unpublished M.Sc. Thesis. National Observatory, Rio de Janeiro, Brazil.

França, A.B., Milani, E.J., Schneider, R.L., O.Lopéz, P., J.Lopéz, M., Suarez, R., Santa Ana, H., Wiens, F., Ferreiro, O., Rosello, E.A., Bianucci, H.A., Flores, R.F.A., Vistalli, M.C., Fernandez-Seveso, F., Fuenzalida, R.P., Muñoz, N., 1995. Paleozoic correlation in South America. In: Tankard, A.J., Suarez, R., Welsink, H.J. (Eds.), Petroleum Basins of South America, vol. 62. AAPG Memoir, pp. 423–444.

Fuentes, R., 1984. Estudio de las temperaturas de la cuenca Marañón, Unpublished Report 300-629-84. Department of Technology, Division of Exploration and Exploitation, Petróleos del Perú.

Fulfaro, V.J., 1996. Geology of Eastern Paraguay. In: Comin-Chiaramonti, P., Gomes, C.B. (Eds.), Alkaline Magmatism in Central-Eastern Paraguay and Relationships with Coeval Magmaitsm in Brazil. University of São Paulo, Brazil.

Golden Software Inc., 2002. SURFER Version 8, Surface Mapping System. Golden Software Inc., Colorado, USA.

Gomes, A.J.L., 2003. Assessment of Geothermal Resources of the State of Rio de Janeiro (in Portuguese), Unpublished M.Sc. Thesis. National Observatory, Rio de Janeiro, Brazil, p. 138.

Gomes, A.J.L. and Hamza, V.M., 2004. Geothermal gradients and heat flow at shallow depths in the coastal area of southeastern Brazil, Brazil. J. Geophys., submitted for publication.

Grigné, C., Labrosse, S., 2001. Effects of continents on Earth cooling: thermal blanketing and depletion in radioactive elements. Geophys. Res. Lett. 28, 2707–2710.

Haenel, R., 1971. Heat flow measurements and a first heat flow map of Germany. J. Geophys. 37, 119–134.

Hamza, V.M., 1982a. Thermal structure of the South American continental lithosphere during Archean and Proterozoic. Revista Brasileira de Geociencias 12, 149–159.

Hamza, V.M., 1982b. Terrestrial heat flow in the alkaline intrusive complex of Poços de Caldas, Brazil. Tectonophysics 83, 45–62.

Hamza, V.M., Muñoz, M., 1996. Heat flow map of South America. Geothermics 25 (6), 599–646.

Henry, S.G., 1981. Terrestrial heat flow overlying the Andean subduction zone, Unpublished Ph.D. Thesis. University of Michigan, Ann Arbour, MI, USA, pp. 194.

Henry, S.G., Pollack, H.N., 1988. Terrestrial heat flow above the Andean subduction zone in Bolivia and Peru. J. Geophys. Res. 93, 15153–15162.

Hertz, N., 1977. Timing of spreading in the South Atlantic: information from Brazilian alkalic rocks. Geol. Soc. Am. Bull. 88, 101–112.

Horai, K., Simmons, G., 1969. Thermal conductivity of rock-forming minerals. Earth Planet. Sci. Lett. 6, 359–368.

Horner, D.R., 1951. Pressure build-up in wells. Proc. Third World Petroleum Congress 34, 316.

Hurter, S.J., 1986. The use of chemical geothermometry and heat loss models in estimating terrestrial heat flow for low temperature hydrothermal systems. Rev. Bras. Geofisica 6, 33–42.

Hurter, S.J., 1992. Heat flow, thermal structure and thermal evolution of the Paraná basin, Southern Brazil, Ph.D. Thesis. University of Michigan, Ann Arbour, pp. 148.

Husson, L., Moretti, I., 2002. Thermal regime fold and thrust belts – an application to the Bolivian sub Andean zone. Tectonophysics 345, 253–280.

Jessop, A.M., Hobart, M.A., Sclater, J.G., 1976. The World Heat Flow Data Collection – 1975, Geothermal Ser. 5. Earth Physics Branch, p. 125.

Kappelmeyer, O., Haenel, R., 1974. Geothermics with Special Reference to Applications. Gebruder Bontraeger, Berlin, p. 238.

Kuhn, C.A., 1991. The geological evolution of the Paraguayan Chaco, Ph.D. Thesis. Texas Technical University, Austin, Texas, p. 185.

Lachenbruch, A.H., Brewer, N., 1959. Dissipation of the temperature effect of drilling a well in Arctic Alaska, Bulletin, 1083-C. U.S. Geological Survey, Washington, USA, pp. 73–109.

Leblanc, Y., Pascoe, L.J., Jones, F.M., 1980. The temperature stabilization of a borehole. Geophysics 46, 1301–1303.

Lindquist, S.J., 1998. The Santa Cruz – Tarija Province of Central South America: Los Monos – Machareti(!) Petroleum System, Open File Report 99-50-C. U.S. Geological Survey, Denver, CO.

Macellari, C.E., 1988. Cretaceous paleogeography and depositional cycles of western South America. J. South Am. Earth Sci. 1 (4), 373–418.

Machado, A., Fontes, S.L., La Terra, E.F., Germano, C.R., Pinheiro, C.A.F., 2001. Electromagnetic studies of the Region of Lakes in the State of Rio de Janeiro – Brazil: tectonic framework and groundwater prospects (extended abstract). International Congress of the Brazilian Geophysical Society, Salvador, BA, pp. 391–394.

Malin, S.R.C., Barraclough, D.R., Hodder, B.M., 1982. A compact algorithm for the formation and solution of normal equations. Comput. Geosci. 8, 355–358.

Mas, L., Mas, G., Bengochea, L., 2000. Heat flow of Copahue geothermal field, its relation with tectonic scheme. In: Proceedings World Geothermal Congress 2000, Kyushu-Tohoku, Japan, pp. 1419–1424.

Mathalone, J.M.P., Montoya, R., 1995. Petroleum geology of the sub-andean basins of Peru. In: Tankard, A.J., Suarez S., R., Welsink, H.J. (Eds.), Petroleum Basins of South America, 62. AAPG Memoir, pp. 423–444.

Middleton, M.F., 1979. A model for bottom-hole temperature stabilization. Geophysics 44, 1458–1462.

Mongelli, F., 1968. Un metodo per la determinazione in laboratorio della conducibilità termica delle rocce. Boll. Geof. Teor. Appl. X, 51–58.

Muñoz, M., Hamza, V.M., 1993. Heat flow and temperature gradients in Chile. Studia Geophys. et Geod., Prague 37, 315–348.

Muñoz, M., Fournier, F.G., Mamani, M., Borzotta, E., 1992. A critical review of magneto telluric studies in diverse tectonic areas in Argentina, Chile and Antarctica. In: Adam, A. (Ed.), Electromagnetic Results in Active Orogenic, Zones, Special Issue Acta, Geod., Geoph, Mont., Hung., Budapest 27, 65–86.

Ocola, L., 1985. Heat flow in Northeastern Peru: Marañon Basin (in Spanish). Third South American Symposium COGEODATA. No., 20, Lima, Peru.

OLADE (Latin American Energy Organization), ICEL, Geotérmica Italian S.R.L. and Contecol, 1982. Reconnaissance study of the geothermal resources of the Republic of Colombia (in Spanish), pp. 1–455.

OLADE – INECEL, ICEL, AQUATER, 1987. Bi-national Geothermal Project: Tulfino-Chiles-Cerro Negro – pre-viability study (in Spanish), vol. 1–5.

Parsons, B., 1982. Causes and consequences of the relation between area and age of the ocean floor. J. Geophys. Res. 87, 289–302.

Pimentel, M.M., Fuck, R.A., Jost, H., Ferreira Filho, C.F., Araujo, S.M., 2000. The basement of the Brasilia fold belt and the Goiás magamtic arc. In: Cordani, U.G., Milani, A.J., Thomaz Filho, A., Campos, D.A.R. (Eds.), Tectonic Evolution of South America, Proceedings of the 31st International Geological Congress, Rio de Janeiro, Brazil, pp. 195–229.

Pindell, J.L., Tabbutt, K.D., 1995. Mesozoic-Cenozoic Andean paleogeography and regional controls on hydrocarbon systems. In: Tankard, A.J., Suarez S., R., Welsink, H.J. (Eds.), Petroleum Basins of South America, vol. 62. AAPG Memoir, pp. 423–444.

Pollack, H.N., Hurter, S.J., Johnson, J.R., 1993. Heat flow from the Earth's interior: analysis of the global data set. Rev. Geophys. 31, 267–280.

Ribeiro, F.B., Hamza, V.M., 1986. Modeling thermal disturbances induced by drilling activity: advances in theory and practice. Brazil. J. Geophys. 4, 91–106.

Robles, D.E., 1988. El gradiente geotérmico en la República Argentina y regiones fronterizas. Boletim de Informaciones Petroleras, 88–95.

Santos, J., Hamza, V.M., Shen, P.Y., 1986. A method for measurement of terrestrial heat flow density in water wells. Rev. Bras. Geofísica 4, 45–53.

Sass, J.H., Lachenbruch, A.H., Munroe, R.J., 1971. Thermal conductivity of rocks from measurements on fragments and its application to heat flow determinations. J. Geophys. Res. 76, 3391–3401.

Sass, J.H., Munroe, R.J., Moses Jr., T.H., 1974. Heat flow from eastern Panama and Northwestern Colombia. Earth Planet. Sci. Lett. 21, 134–142.

Sass, J.H., Priest, S.S., Duda, L.E., Carson, C.C., Hendricks, J.D., Robison, L.C., 1988. Thermal regime of the State 2-14 well, Salton Sea Drilling Project. J. Geophys. Res. 93 (B11), 12995–13004.

Schwarz, G., Chong Diaz, G., Kruger, D., Martinez, E., Massow, W., Rath, V., Viramonte, J., 1994. Crustal high conductivity zones in the southern central Andes. In: Reutter, K.J., Scheuber, E., Wigger, P. (Eds.), Tectonics of the Central Andes. Springer, Berlin, pp. 49–67.

Shen, P.Y., Beck, A.E., 1983. Determination of surface temperature history from borehole temperature gradients. J. Geophys. Res. 88, 7485–7493.

Simpson Jr., S.M., 1954. Least-squares polynomial fitting to gravitational data and density plotting by digital computers. Geophysics 19, 1283–1289.

Smith, L.R., 1989. Regional variations in formation water salinity, Hollin and Napo formations (Cretaceous), Oriente basin, Ecuador. Am. Assoc. Petroleum Geol. Bull. 73, 757–776.

Springer, M., 1999. Interpretation of heat flow density in the Central Andes. Tectonophysics 306, 377–396.

Springer, M., Foerster, A., 1998. Heat flow density across the Central Andean subduction zone. Tectonophysics 291, 123–139.

Stein, C.A., Stein, S., 1992. A model for the global variation in oceanic depth and heat flow with lithospheric age. Nature 359, 123–129.

Steinmuller, K., 2001. Modern hot springs in the southern volcanic cordillera of Peru and their relationship to Neogene epithermal precious – metal deposits. J. South Am. Earth Sci. 14, 377–385.

Swanberg, C.A., Morgan, P., 1979. The linear relation between temperature based on silica content of groundwater and regional heat flow: a new heat flow map of the United States. Pure Appl. Geophys. 117, 227–241.

Tschopp, J.L., 1953. Oil explorations in the Oriente of Ecuador, 1938–1950. Bull. Am. Assoc. Petrol. Geol. 37, 2303–2347.

Uyeda, S., Watanabe, T., Kausel, E., Kubo, M., Yashiro, Y., 1978. Report of heat flow measurements in Chile. Bull. Earthquake Res. Inst. Tokyo 53, 131–163.

Van den Beukel, J., Wortel, R., 1987. Temperature and shear stresses in the upper part of a subduction zone. Geophys. Res. Lett. 14, 1057–1060.

Van den Beukel, J., Wortel, R., 1988. Thermo-mechanical modeling of arc-trench regions. Tectonophysics 154, 177–193.

Vasseur, G., Nouri, Y., 1980. Trend of heat flow in France: relation with Deep Structure. Tectonophysics 65, 209–223.

Vitorello, I., Hamza, V.M., Pollack, H., 1980. Terrestrial heat flow in the Brazilian highlands. J. Geophys. Res. 85, 3778–3788.

Von Herzen, R.P., Maxwell, A.E., 1959. Measurements of thermal conductivity of deep-sea sediments by a needle-probe method. J. Geophys. Res. 64, 1557–1563.

Watanabe, T., Uyeda, S., Guzman Roa, J.A., Cabre, R., Kuronuma, H., 1980. Report of heat flow measurements in Bolivia. Bull. Earthquake Res. Inst. Univ. Tokyo 55, 43–54.

Wessel, P., Smith, W.H.F., 1992. The GMT-System version 2.1, Technical Reference and Cook-book. School of Ocean and Earth Science and Technology, University of Hawaii, Hawaii, USA.

Wiens, F., 1995. Phanerozoic tectonics and sedimentation in the Chaco basin of Paraguay, with comments on Hydrocarbon Potential. In: Tankard, A.J., Suarez S., R., Welsink, H.J. (Eds.), Petroleum Basins of South America, vol. 62. AAPG Memoir, pp. 185–205.

Zalan, P.W., 1987. Tectonics and sedimentation of the Paraná Basin (in Portuguese). In: Proceedings of the Third South Brazilian Symposium on Geology, Curitiba, PR, pp. 38–67.

Zeng, H., 1989. Estimation of the degree of polynomial fitted to gravity anomalies and its application. Geophys. Prospect. 37, 959–973.